Joana Margarida Coimbra de Matos

New Precipitated Calcium Carbonate Derived Structures For Application In Papermaking

Master Thesis in Chemical Engineering supervised by Doctor Paulo Jorge Tavares Ferreira and Engineer António Paulo Mendes de Sousa and submitted to the Department of Chemical Engineering, Faculty of Science and Technology, University of Coimbra

2017

· U · C ·

UNIVERSIDADE DE COIMBRA

Cover Photo: Modified PCC with citrate buffer – FESEM image with magnification 20k x.

Joana Margarida Coimbra de Matos

New Precipitated Calcium Carbonate Derived Structures For Application In Papermaking

Dissertation submitted to the Department of Chemical Engineering,
Faculty of Science and Technology, University of Coimbra

Supervisors

Doctor Paulo Jorge Tavares Ferreira

Engineer António Paulo Mendes de Sousa

Institutes

Chemical Engineering Department of University of Coimbra

RAIZ – Research Centre of Forest and Paper

Coimbra,

· U   C ·

UNIVERSIDADE DE COIMBRA

The very nature of science is discoveries,

and the best of those discoveries are the ones you don't expect.

Neil deGrasse Tyson

Acknowledgements

During the execution of the current thesis, I could count on several supports that helped me to reach this goal. To the people that played an important role in this journey, I want to express my special thanks.

I would like to thank my advisor Professor Doctor Paulo Ferreira, that even with short available time, supported and guided me throughout this work.

To Engineer António Paulo Mendes de Sousa, co-advisor in this work for the support given during my presence in RAIZ.

To Engineer Ana Filipa Lourenço for all the support during the beginning of my work and for being available to think together on several solutions. Also, for convey me rigor in all the tasks to be performed. I wish you all the joy of the world in this new chapter of your life!

To the recent graduate Engineer Diana Godinho, thank you for all the support and help! You were a fundamental card in the final part of this project.

I would like to thank RAIZ and its employees, for all the help and support given during my time there. To Engineer Jorge Pedrosa for guiding me during print quality tests and to his colleagues for providing all those happy moments.

To my colleagues from B27 and B29 for always helping me when I needed and for always have a "playing time" during the most tiring days.

To my friends that during my journey showed me support and had always a friendly word to say. Isabel Gonçalves, Marta Batista, Rafael Torres, thank you for being always there when I needed.

To the family that Coimbra gave me: Ana Rita Varelas, Célia Pedro, Daniel Marcos, Joana Azevedo, Margarida Fernandes, Pedro Sobral and Sara Costa. I thank you for being always with me even when the physical separation is an obstacle. Throughout these pass months life was not so good with some of us, but we showed that together all those bad moments became easier to face.

To my parents and brother, the most special thank you! For always believing in me and providing me all the opportunities of my life. Without you none of this would be possible.

Abstract

In a previous work a strategy with citrate buffer used to deconstruct the paper matrix of commercial printing and writing paper with the objective to isolate its mineral loading resulted in the discovery of lamellar particles, interesting from a papermaking point of view. This led to a complementary study, where industrial scalenohedral PCC (Precipitated Calcium Carbonate) particles contacted with the citrate buffer, confirming that in fact the origin of the lamellar structures is related to it.

This dissertation aims to study and optimize the conditions of the reaction between the citrate buffer and the mineral particles. To understand which variables influence this PCC modification and later apply these particles as coating pigment and paper filler to evaluate the resultant properties, are also objectives of the work.

A preliminary research was made where the influence of the pH buffer and CIT (Citric Acid)/PCC ratio was studied, at 50ºC. From this experimental investigation resulted two new protocols to have a better control of CIT/PCC ratio. Also, an experiment using GCC as starting material was made. From this approach, it was concluded that the lamellar particles are favourable to form in a suspension with pH 5.5. The CIT/PCC can be controlled by the different protocols, where a solution of CIT (1M) is added to the PCC suspension or two distinct solutions of CIT (1M) and NaOH (1M) are added separately until the optimum pH is reached. The modification of GCC particles did not present lamellar morphology, but a platy/rounded one.

These particles were subjected to thermal analysis (calcination and TGA up to 900 ºC) revealing that calcium citrate is its major component, ca. 30% is $CaCO_3$ and 10% are unidentified compounds. The size of the particles was measured by the LDS technique, revealing that the modified particles are smaller than the starting material, having an average size of 3.30 – 3.50 µm. The modified particles obtained from GCC present higher size than its original one. Relatively to the particles surface charge, it was found the new structures are highly negative.

The modified particles were applied as paper pigment coating. The coatings with the pigments produced with citrate buffer exhibited higher optical density and higher gamut area values when compared with the paper base, revealing promising results of these particles in increasing paper printing quality. Contrarily, the PCC particles modified only with a CIT solution and all GCC modified particles, did not present results as good as the previous.

From the application of these particles into the paper matrix resulted sheets with lower filler content. For this reason, conclusions about the influence of these fillers in the paper properties are not possible. Further studies are needed related with the retention agent, and the possible tendency of the particles to flocculate.

Key-words: Lamellar; Precipitated Calcium Carbonate; Sodium Citrate; Fillers; Pigment; Paper.

Resumo

A partir de estratégias de dissolução da matriz fibrosa presente no papel de impressão e escrita, recorrendo a tampão citrato, com o objetivo de separar o material inorgânico, resultaram estruturas lamelares interessantes do ponto de vista papeleiro. Este estudo realizado num trabalho anterior, levou a um outro estudo complementar: foi adicionado tampão citrato ao PCC (Carbonato de Cálcio Precipitado) escalenoedro industrial, provando assim a origem destas estruturas.

A presente dissertação tem como objetivo o estudo e otimização da reação que ocorre entre o tampão citrato e as partículas minerais. Pretende-se também entender que variáveis influenciam a modificação do PCC. Posteriormente, a aplicação destas partículas como pigmento de revestimento do papel e *filler* é avaliada pelas propriedades obtidas.

Num estudo preliminar foi estudada a influência do pH do tampão citrato e a razão entre ácido cítrico e partículas de carbonato de cálcio (CIT/PCC) à temperatura de 50 ºC. Desta investigação resultaram dois novos protocolos com o objetivo de ter um melhor controlo da razão CIT/PCC. Foi também realizada uma experiência usando GCC como material de partida. Desta abordagem conclui-se que as partículas lamelares se formam favoravelmente quando a suspensão se encontra a pH 5,5. A razão CIT/PCC pode ser controlada pelos diferentes protolocos criados onde uma solução de ácido cítrico (1M) é adicionada à suspensão de PCC, ou quando duas soluções distintas de CIT (1M) e NaOH (1M) são adicionadas separadamente até que o pH ótimo seja atingido. Da modificação das partículas de GCC resultaram partículas com morfologias semelhantes a uma moeda.

Da análise térmica destas partículas (calcinação e TGA até 900 ºC) conclui-se que as amostras têm como maior constituinte citrato de cálcio, cerca de 30% de $CaCO_3$ e 10% de compostos que não foi possível identificar. A análise à energia de carga superficial revelou que as partículas modificadas são eletricamente negativas.

As partículas foram aplicadas como pigmento de revestimento. Dos revestimentos onde foram usadas partículas modificadas com tampão citrato, obtiveram-se valores de densidade ótica elevados, resultando por consequência em valores que área gamut superiores aos obtidos no papel base usado. Este facto revela resultados promissores na aplicação destas partículas para o aumento da qualidade de impressão. As partículas modificadas apenas com solução de CIT e as resultantes da modificação de GCC não apresentaram resultados tão bons como os anteriores.

A aplicação destas partículas na matriz do papel não foi bem sucedida uma vez que resultou na formação de folhas com pouca percentagem de *filler*. Por esta razão, não podem ser tiradas conclusões acerca da influência que estas partículas podem ter nas propriedades do papel. Posteriormente, será necessário fazer-se estudos relacionados com o agente de retenção usado e sobre a possível tendência das partículas para flocular.

Palavras-Chave: Lamelar; Carbonato de Cálcio Precipitado; Citrato de Sódio; Cargas Minerais; Pigmento; Papel.

Contents

List of Figures

List of Tables

Nomenclature

Acronyms:

ACC	Amorphous Calcium Carbonate
B&W	Black and White
BP	Base Paper
CIT	Citric Acid
CMYK	Cyan, Magenta, Yellow, and Black
CPAM	Cationic Polyacrylamide
CTAB	Cetyltrimethylammonium Bromide
DOD	Drop-On-Demand
DSC	Differential Scanning Calorimetry
EDTA	Ethylenediaminetetraacetic Acid
ELS	Electrophoretic Light Scattering
FESEM	Field Emission Scanning Electron Microscopy
GCC	Ground Calcium Carbonate
IPN	Pedro Nunes Institute
ISO	International Organization for Standardization
LDS	Laser Diffraction Spectrometry
LWC	Light Weighted Coated
MA	Malic Acid
OBA	Optical Brightening Agents
OM	Optical Microscopy
P&W	Printing and Writing
PAA	Polyacrylic Acid
PCC	Precipitated Calcium Carbonate
PEG	Polyethylene Glycol
pKa	Dissociation Constant
PSD	Particle Size Distribution
PVA	Polyvinyl Alcohol
RAIZ	Research centre of Forest and Paper
SC	Sodium Citrate
TAPPI	Technical Association of the Pulp and Paper Industry
TGA	Thermogravimetric Analysis

Greek Letters

α	Alfa
ζ	Zeta Potential

1   Introduction

1.1   Motivation and Objectives

Mineral fillers, which are paper functional additives, can be found in different types of paper, being mostly used on printing and writing paper grades.

These minerals have several properties (such as morphology, size, surface area, and brightness and chemical composition) that improve paper properties such as optical properties, bulk (specific volume of the paper), smoothness, and printability. Besides, since fibers are replaced by mineral fillers, these have also a very positive impact on the economy of the paper making process.

Mineral particles can represent 20 to 30% of the paper composition, and higher values are uncommon because fillers disrupt the fiber network, so disturbing some mechanical properties such as tensile strength and stiffness (Hubbe and Gill, 2016).

In this scenery, for benchmarking and reverse engineering reasons, it is of utmost importance to access the content and structure of the fillers in the paper sheets, and this requires the deconstruction of the fiber matrix without damaging the fillers, as much as possible.

In a previous work, different strategies to deconstruct the fibrous matrix of commercial printing and writing papers (P&W) were studied, aiming at isolating the mineral fillers without their degradation. In this work, a biological solvent containing citrate buffer was used, among other chemical treatments, and as a result particles of PCC (Precipitated Calcium Carbonate) with an interesting lamellar shape were obtained, as revealed by FESEM (*Field Emission Scanning Electron Microscopy*).

This discovery led to a complementary study on what effect could this buffer have on the industrial PCC particles. It was confirmed that the citrate buffer can change the scalenohedral original PCC shape to a lamellar one. This kind of structure may have a positive impact on paper properties when used as filler or also as a pigment coating.

In this context, the present work was developed with the objective of optimizing the conditions of the reaction between the citrate buffer and the mineral particles, and also of evaluating the resultant mineral structure and its influence on paper properties (both when used in the matrix or at the surface as pigment coating).

1.2   Thesis Structure

This dissertation is divided into the following chapters:

- <u>Chapter 1</u>: Introduction

This chapter serves to explain the purpose of the study and how it was structured.

- <u>Chapter 2</u>: Literature Review

In this chapter, a theoretical framework about papermaking and paper coating is presented. Also, an approach about paper fillers and coating pigments is also made. Furthermore, a reference about the interaction between PCC and organic compounds is reviewed and a more detailed description about its interaction with citric acid is examined.

- <u>Chapter 3</u>: Materials and Methods

This chapter describes the materials and methods used in this work, with the aim that the obtained results can be reproduced by others.

- <u>Chapter 4</u>: Results and Discussion

The results related with the particles characterization, and their application as paper coating pigment and filler are presented and discussed in this chapter.

- <u>Chapter 5</u>: Conclusions

The conclusions that resulted from the previous chapter are summarized.

- <u>Chapter 6</u>: Future works

Several suggestions of work that was not possible to perform in the present study are given.

- <u>Appendices</u>:

This chapter includes data and information that could be important for better understanding of the present work.

2 Paper and Papermaking

In a broader definition, paper is a suspension of cellulosic fibers, properly mixed and prepared to form stable bonds with each other that can originate a structure able to support traces and stains or used as packaging material as well as other specific applications. The fibrous suspension is essentially originated by plants, and additives can be added to it. The final sheet is formed after the elimination of water through the mesh of the web and successive drying.

Paper applications are very vast, however printing and writing (P&W) papers are the most widely used, and wood is the main cellulosic source.

In the papermaking process, wood is used as a renewable raw material that comes from well managed forests. The process starts by debarking and chipping the wood. Then the pulp manufacture can be done by mechanical or chemical methods, depending on the desired final sheet. Chemical pulping is the most used process to obtain high quality printing papers and its objective is to remove the lignin components without destroying the cellulosic fibers. In this stage, wasted paper for recycling (after de-inking) and broke (paper trimmings and paper that must be reprocessed in the mill) can be added to the mixture.

The next step is refining and it is one of the most important operations since it determines some physical properties and the quality of the final sheet - it increases the apparent density of the paper (Hubbe and Gill, 2016). Here, fibers suffer mechanical action (such as tensile, compressive, shear and bending forces) that opens up and divides them, increasing their surface area and consequently improving the fiber bonding. Before heading to the paper machine, fibers are washed and screened. Chemical additives can also be added, including dyes and pigments, and also fillers (Bajpai, 2015).

The stock is fed into the paper machine and water is removed forming the paper web, initially with the consistency of 0.1%. The sheet is formed in the wire section where water is drained through the mesh and fibers are aligned in the machine direction. Vacuum boxes located under the wire also help the water drainage. After this, paper undergoes compression, to squeeze out more water, and drying, where the remaining water (4-6%) is removed by evaporation. This last step, despite only removing a small amount of water, is the most expensive one as it requires high energy. The forming paper reaches the consistency value of 97%.

At the end of the paper machine, the paper is rolled up and cut with the desired diameter. Depending on the purpose of the paper, the process is now finished or it will require other operations such as coating, calendaring and winding.

The coating step is usually done in papers that demand high quality and brightness. The coating layer is added to the base paper that was produced in the paper machine, and it is

composed by pigments (eg. clay, calcium carbonate), binders (starch) and other additives such as polymers and optical brighteners (Biermann, 1996). Binders are used to ensure that the filler material connects with the paper surface, forming a cohesive layer. This operation improves, not only the uniformity of the paper but also the smoothness and brightness of the base paper. It also has an important role in the printing process, since it refines the resolution of printed images, improving the gloss of the film and decreasing the show-through, keeping the ink into the paper surface.

An on-machine process called calendaring follows the previous step, where the paper passes by a series of polished steel rolls. Here the irregularities in the sheet are reduced, improving the smoothness and creating a sheet with higher density.

2.1   Paper fillers

As it was previously said, the paper is not made only of cellulosic fibers and that happens because the fibers themselves do not comply the requirements of the final customer, with the regard to opacity, in typical grades of printing papers, at lower values of basis weight (mass per unit of area). Thus, the use of mineral loading gives the papermaker several ways to meet customer needs and profitability. Also, to aid the process of papermaking and to improve the finished sheet, various types of fillers and additives are added to the pulp before formation (Hubbe and Gill, 2016).

In terms of additives, they can be classified as functional and control additives. The first type includes dyes, internal sizing agents, adhesives, and fillers; the second one refers to biocides, drainage and retention aids and defoamers, and they do not affect the final paper directly and are not necessarily retained on it (Biermann, 1996).

Fillers, by definition, are water insoluble substances with size magnitude of 0.1 to 10μm dispersed into the slurry before paper formation (Hubbe and Gill, 2016). Being the second ingredient with the major percentage in the paper, fillers have dominant application in P&W papers. There are several reasons for its use, one of them is to reduce the cost of paper production, where the increase of 1% in loading material saves approximately $2.50/ton in feedstock and energy costs. This cost reduction is due to the drainage and drying improvement (energy savings), and to the use of less virgin pulp, since the capacity of paper production can be increased with the use of mechanical pulp (with low quality) and recycled pulp (Hu, Shao, Li, *et al.*, 2009; Bajpai, 2015).

The filler shape is an important factor to have in consideration, since it affects the light scattering properties, the calendaring process, the drying rate, and the air permeability of the paper (Biermann, 1996). In terms of shape, they can be classified as "platy", where are included clay, talc, and mica, or as "blocky", such as ground calcium carbonate (GCC) (Hubbe and Gill, 2016).

Depending on the filler size distribution, fillers can have different behavior if applied as a coating or bulk material. In the coating process, a wide particle size distribution can be an advantage, as the particles join together forming a dense layer (Hubbe and Gill, 2016). However, as paper filling, a uniform particle size distribution has a better impact. Besides it, in this context, the mineral length is a key factor, since particles with a larger diameter may not be retained in the matrix due to their decreased specific surface area. On the contrary, smaller particles have a higher surface area but they compete with the sizing agent, being difficult to give internal sizing to the final sheet (Biermann, 1996).

Among other reasons, mineral loading contributes to improving the paper formation since it fills the empty spaces around the fibers. For this reason, the inorganic material provides the sheet a more uniform and a smoother surface, increases the opacity and brightness and enhances the printability (the show through is decreased and the receptivity to ink is increased) (Au and Thron, 1995; Jimoh, Ariffin, *et al.*, 2017).

It is obvious that, depending on the interaction of the filler with inks, glues, or other polymers, applied to the paper surface, the final product can be differentiated. So, a detailed knowledge of the mineral composition and morphology can be helpful to the papermaker to evaluate the pros and cons of the use of a certain filler.

2.2   Coating process

The coating process is commonly used in the papermaking industry to improve the appearance and printability of the paper. The base paper is rough and difficult to cover with a thin coating layer. For printing methods it is required that the coating layer is homogeneous and covers the substrate. The desired properties for a coated paper are usually high brightness and high gloss. Although, this step increases the production cost and is therefore mainly used when the appearance of the product is of great importance.

In paper coating, an aqueous suspension is applied to the base paper surface, filling the uneven spaces, and covering the highest lying fibers as possible. The size of the covering layer

is influenced by its density: for the same weight, a coating with low density has a greater covering area than a coating with high density. It can be done in one side, or in both sides of the sheet. After, the paper is dried and finished, achieving the gloss and smoothness required.

The suspension used for the coating is a mixture of water with white pigments (eg. clay, calcium carbonate, talc and titanium dioxide) and binders (eg. starch and latex). Some additives can be added to influence the solid content, rheology and water retention, such as dispersants and thickeners. The coating layer consolidates as water evaporates, allowing the binder to form bridges between the pigment particles and the base paper. This suspension should only contain the necessary amount of water to ensure flow properties, in order to save energy and costs for drying. In the industrial coating, the solid content is about 70wt%.

As one of the purposes for coating paper is to enhance the printability, the coating layer should be strong enough to resist the stress of the printing process, thus there is an allowable minimum amount of binder that can give the necessary strength to the coating. However, when the suspension has excess of binder, it can have a negative effect on the coated paper such as low opacity and gloss, as well as glueability problems.

The industrial coating technique is in constant evolution to comply with the demands for high quality and faster production. The most common coating processes used are applicator rolls (also called dip coater) and jet applicators (Figure 1). In these methods, an excess of coat is applied to the substrate that is after measured with the desired coat weight (Ek, Gellerstedt and Henriksson, 2009). In the first method, the suspension is transferred from a bin to the substrate which is supported by a large backing roll. The amount of coating transferred to the substrate is influenced by the distance between the backing roll and the applicator, the speed of the applicator, and by the viscosity of the mixture. The jet applicator applies the coating suspension on the paper surface through a nozzle and here, the coating transfer is controlled by the width of the opening, the pressure of the jet and the angle of the applicator to the moving paper web.
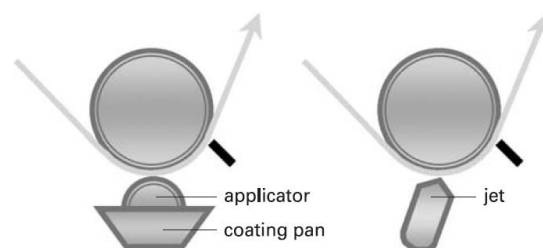

Figure 1. Coating process: Applicator Roll (left) and jet applicators Adapted from (Ek, Gellerstedt and Henriksson, 2009)

In laboratory studies, the coating process is made with a bench coater, an equipment very easy to handle. This coater uses a rod placed on the top of the substrate which is attached to a holder that moves the rod over the substrate at a given speed. The coating suspension is applied manually in front of the rod and then is transferred to the substrate by the gap between the rod and the paper surface. The excess of coating is pushed forwards by the moving rod until the end of the paper base. The thickness of the coating layer is controlled not only by the distance between the rod and the surface, but also by the kind of rod used.

When the coating is applied in the paper, the water is absorbed into the paper and the natural evaporation helps to promote the drying process. However, the absorption of water must be allowed in the shortest time as possible to preserve the dimensional and strength properties of paper. To speed up the drying process the coated paper is dried by means of air or infrared (IR) dryers. The last ones can remove water more efficiently than the air dryers, and for that reason are the most used dryers.

The properties of the final coated paper can be improved by the calendering process, producing a surface suitable for printing. Here, the paper undergoes compression in one or more rolling nips, reducing the roughness of the surface. These rolls can be heated or have a higher line load to increase the compression. However, in this treatment, the temperature has high impact in the increasing of gloss and decreasing of roughness. Besides its positive effects, calendering promotes the decreasing of the opacity and brightness of the coating layer.

2.3   Pigments

The pigment particles in the coating layer represent about 85-95wt% of the coating layer, and its properties influence not only the coating layer formation but also the calendaring process. The coating mixture must be able to flow during the application and should cover all the paper fibers. Because of the last reason, coarse and platy particles as well as high coat weights are often used in the mixture; also, the minerals used are white pigments to hide the fibers and thus allowing the improvement of brightness, whiteness, opacity, and smoothness.

The cost of the coating is determined by the pigment used, and the more commonly used are calcium carbonates and kaolin. These pigments are usually from natural origin and are physically and chemically homogenous; their properties (such as particle size and distribution, particle shape, refractive index, light scattering, light absorption, and density) can affect the final appearance of the coating as it can be seen in Table 1 (Holik, 2013; Bajpai, 2015).

The largest dimension of a pigment is defined as its aspect ratio and gives the platiness of the pigment, responsible for the properties of the coated paper such as gloss and porosity of the surface (Holik, 2013). Those pigments are often agglomerates or aggregates of many particles, which can be difficult to measure in size. For that reason there are techniques, such as laser light diffraction that provide the particle size distribution (PSD) of equivalent spherical particles, however it can be used as comparative methods for particles with other shapes. A narrow PSD has very small and very large pigment particles, which leads to a more porous structure of the coating layer, contributing strongly to optical properties such as increasing of gloss and brightness. However finer particles promote higher gloss and lower roughness of coatings (Caner, Farnood and Yan, 2006).

Table 1. Influence of pigment properties on coating

Increased platiness and /or particle size	Better gloss development
Increased refractive index and /or particle size	Higher opacity
Decrease in light absorption	Higher brightness
Decrease in packing	Higher porosity and better ink absorption
	Higher bulk and better coverage

2.3.1   Printing process and printing quality

Printing properties are dependent on the coating process, since this treatment enhances the paper surface properties, and can make it suitable to receive ink. The objective of printing is to reproduce texts and coloured pictures using cyan, magenta, yellow, and black inks (CMYK). Nowadays, the processes used for printing proposes are the technologies of offset, flexographic and rotogravure printing. In addition, digital printing process, such as inkjet and xerography, are also widely used (Holik, 2013). The process used in the present work is the inkjet printing, and for that reason, this section will be relative to it.

In the inkjet printing the image formed directly on the substrate is controlled by digital data. For this reason, this system can work with a large variety of inks and is able to print several kinds of data. Inkjet papers are usually coated by starches, polyvinyl alcohol (PVA), polymers, and pigments. This is mostly made to enhance the whiteness and the inks' receptivity to the surface (Mesic and Johnston, 2013).

It is a contactless printing process, which means that it can be used in several types of substrates. The ink passes from a reservoir and can be propel onto the paper in two distinct ways: drop-on-demand (DOD) and continuous inkjet. In the DOD inkjet, the ink droplets are expelled from the reservoir, directly to the paper, due to a pressure change created by a heating element or a piezoelectric element. In continuous inkjet, a continuous flow of ink is created by means of a pump, and with help of the vibration of piezoelectric crystals, it is broken into individual droplets. This droplets are then charged and subjected to an electrostatic field, controlling this way their direction to a specific point (Singh *et al.*, 2010).

The print quality is influenced by the ink properties (surface tension and viscosity), which control the droplet spreading, and by the substrate's absorption properties, such as roughness, surface tension and porosity (Martin, 2005). The inks used in this printing process are normally composed by an aqueous solvent that serves as a vehicle for dyes and pigments to disperse evenly.

Despite the fact that the ink needs to be rapidly immobilized onto the paper surface, its high absorbency can lead to print-through and poor optical density. However, if the absorption process takes more time than the desired, it may spread laterally resulting in colour-to-bleed. To have the pretended printing quality properties, it is the major importance to control ink spreading, holdout and its penetration in the paper; the paper opacity is also an aspect to be taken into account.

The printing quality requires the evaluation of its parameters with high exigency. Printability results from the complex interactions between the ink, the printing process, and the paper. The sheet must be able to accept evenly the solids of the ink, without the formation of irregular films and stains (Bajpai, 2015).

The evaluation of the printing quality should be made with methods able to quantify numerically its parameters. These tests evaluate the uniformity, definition, contrast and optical density. Some important aspects related to these properties are:

- Mottling: stained pattern observed in a printed sheet.

- Colour-to-colour bleeding: measure the mixture between two adjacent colours. This parameter is related to the lateral spreading of the ink to an adjacent area where another colour was printed. This phenomenon is due to low ink absorption in the paper, leading to higher drying time, and increasing the risk of blending between the two colours.

- <u>Optical Density</u>: it is dependent on the amount of ink that penetrates in the paper. It is given by the relation between of light reflected from a paper sheet before and after printing. A higher optical density corresponds to a thicker film of ink, resulting in higher colour intensity (Moutinho, Ferreira and Figueiredo, 2007).

- <u>Gamut area</u>: this value translates the paper's ability to reproduce colours. It is given by the area on a hexagon whose vertices correspond to the pairs (a*, b*). These values are integrated on the coordinated system CIELab, which uses the colour coordinates L* (luminosity), a* (measure of shade in the red/green axis), and b* (measure of shade in the yellow/blue axis). The positive values of a* and b* are the correspondent colours of red and yellow (Moutinho, Ferreira and Figueiredo, 2007). A representation of this can be seen in Figure 2 .
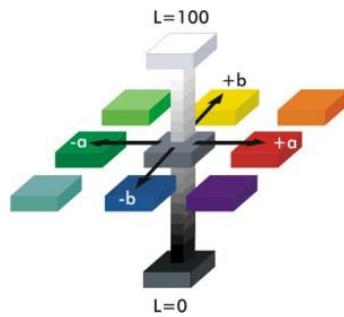
Figure 2. CIELab Coordinates

- <u>Print-through</u>: is relative to the ability to see a printed image on the opposite side of the sheet. It is calculated with the chromatic coordinates L*, a* and b*, and influenced by the pigment/dye penetration.

- <u>Show-through</u>: depends on the quantity of pigment/dye that is retained at the paper surface. It is also calculated with the chromatic coordinates L*, a* and b*, and it is evaluated laying a sheet above the printed one, evaluating the ability to see the printed image through it.

Another important aspect of the printing process is the runnability. This parameter is influenced by the strength properties of the paper and corresponds to the velocity that the paper passes through the printing machine without causing disturbs and stops (Bajpai, 2015).

2.4 Inorganic materials most used in the papermaking process

The loading material used onto the paper can be distinguished in two different groups, organic and inorganic. The organic fillers are mostly used in speciality papers or coated P&W papers. However, due to their high cost, they are not used in all paper grades. In this group are included polymers, starch derivatives, and resins. The inorganic fillers are the most widely used in the papermaking process, since they confer great properties to the paper at low cost.

As it was said before, the main objective of the present thesis is to study the new material found in a previous work based on reverse engineering, where the main goal was to isolate the inorganic fillers contained in the matrix of commercial printing and writing paper, without their degradation (Carecho, 2016).

To better understand some characteristics of this new material, it is important to know in advance which are the inorganic fillers most used in the papermaking process, as loading fillers and as a coating pigments.

As shown in Figure 3, in terms of quantities applied and global demand in the papermaking filler market, the main loading material used are calcium carbonates (64%, where 49% is GCC and 15% is PCC), followed by kaolin (29%), titanium dioxide (1%), and talc and other pigments (6%) (Nutbeem, 2013; Bajpai, 2015).
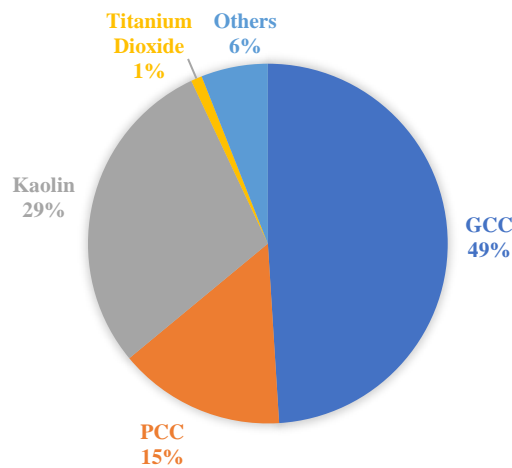
Figure 3. Fillers demanding market (Bajpai, 2015)

A coated paper is characterized for its excellent printability, esthetical attractiveness and a valuable feel. Most of the pigments used in coating are cheaper than chemical pulps, and their use represents a very important economic factor. Figure 4 shows the global consumption of the inorganic materials used as pigments, where it can be highlighted the use of calcium carbonates (76%) and kaolin (20%) as the minerals with highest demand market (Nutbeem, 2013). Nowadays the use of calcium carbonate is increasing and talc is showing constant growth, whereas kaolin is stagnating (Bajpai, 2015).
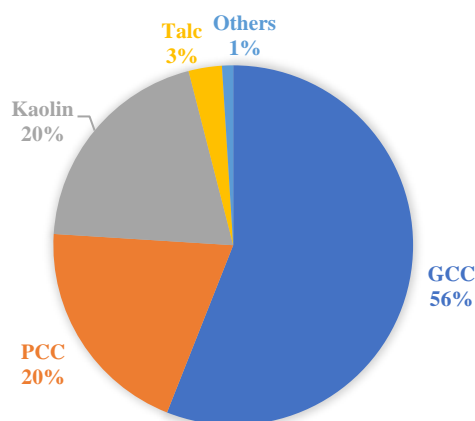
Figure 4. Pigments demanding market. Adapted from (Nutbeem and Nutbeem, 2013)

There are some important characteristics of the pigment that are very relevant from a papermaker's perspective such as colour, brightness, opacity power (given from their scattering coefficient) and, of course, its cost. Usually, the fillers with the highest optical performance have the smallest particle size, and the highest refractive index, brightness and scattering coefficient. Table 2 summarizes typical values for the minerals mentioned before and the following topics give a brief description of these materials and their properties that will influence in the papermaking process (Holik, 2013; Hubbe and Gill, 2016). More importance will be given to PCC, since it was the starting material of the new particles in study in this work.

Table 2. Typical properties of the most used fillers in papermaking. Adapted from Hubbe and Gill (2016), Bajpai (2015), Holik (2013)

Filler	Types	Morphology	ISO Brightness (%)	Refractive index	Mean diameter (µm)	Density (g/cm³)	Specific Surface Area (m²/g)
Kaolin	-	Platy	$70 - 90$	1.56	$2 - 5$	2.6	$10 - 20$
Talc	-	Platy	$70 - 88$	1.58	$1 - 20$	2.7	$5 - 20$
TiO2	Rutile	Rounded	$97 - 99$	2.75	$0.2 - 0.35$	4.2	$8 - 12$
	Anatase	Rounded	$97 - 99$	2.55	$0.3 - 0.35$	3.8	$8 - 12$
Calcium Carbonate	Natural	Rhombohedral	$80 - 96$	1.58	$0.8 - 2$	2.7	$2 - 12$
	Precipitated	Scalenohedral; Aragonite; Rhombohedral; clustered or agglomerated	$92 - 99$	1.56	$0.8 - 2$	2.7	$4 - 12$

2.4.1 Kaolin

Kaolin, $Al_4(OH)_8(Si_4O_{10})$, is a white silicate material that can be found in sedimentary and metamorphic deposits, and it is formed by decomposition of granite. It has a platy morphology and it is predominantly used in uncoated papers. This almost inexpensive mineral has desirable optical properties when used as filler, since it lowers the porosity of the sheet increasing the gloss of the finished paper after calendaring (Holik, 2013; Bajpai, 2015; Hubbe and Gill, 2016).

Nowadays, kaolin remains a major resource in papermaking as a wet-end additive and as a coating pigment. The growth of the supercalendered paper market raises the need of higher brightness in the sheets, which promotes the continuous use of kaolin. This is due to its natural shape that, when used for fiber coverage, leads to paper and printing gloss. Also, mixing this pigment with GCC, PCC and talc can lead to a better performance (Bajpai, 2015).

The coating pigment is mixed with water and binder, and applied to a paper substrate by means of a high speed blade coater (Bundy and Ishley, 1991). Its particle shape with higher aspect ratio and its high brightness are the most appealing properties for application in the base paper. After calendering, the particles tend to orient parallel to the surface promoting both proper smoothness and gloss, giving an optimal ink receptive surface (Bundy and Ishley, 1991; Caner, Farnood and Yan, 2006; Ek, Gellerstedt and Henriksson, 2009).

2.4.2 Talc

Talc, $Mg_3Si_4O_{10}(OH)_2$, is a layered silicate with a platy morphology. The layers of this mineral are electrostatically neutral resulting in a mineral strongly oleophilic. However, due to its surface properties, talc is known as a detackifier and used a pitch controller in the papermaking process. This inert mineral is also characterized by its softness and for being organophilic (helping to reduce dye consumption and two-sidedness in the coloured paper) (Gane and Ag; Bajpai, 2015; Hubbe and Gill, 2016).

When used as a filler, this mineral contributes to paper hydrophobicity and uniformity of colour in both sides of the sheet. Due to their relatively large particles and water resistant particles, this mineral improves dewatering in the papermaking process, it leads to higher retention in the sheet and lowers the papers' strength properties. The pitch control function leads to a better runnability of the paper machine. Speaking in the paper quality itself, the use of talc increases the smoothness, gives better printability (especially in rotogravure papers), deeper colour in coloured papers, and has a lower impact on strength properties than other fillers (Holik, 2013; Bajpai, 2015).

Talc is used nowadays in light weighted coated paper (LWC) and coated fine papers in offset formulations. As coating pigment, since talc has a low coefficient of friction due to the low cohesion that exists between the crystal layers inside the talc particles, it reduces paper breaks, even when subjected to constant tension (Holik, 2013). The properties of the coating can improve some properties such as smoothness, coarseness peeling resistance and ink absorption. However, talc tends to reduce gloss and prolong the ink drying time. It is also said that if a composite of talc and silica is used as coating pigment, it enhances the quality of the printed images better than when used as a single pigment (Lin *et al.*, 2016).

2.4.3 Titanium Dioxide

Titanium dioxide, TiO_2, is a speciality filler and it has the highest brightness, density and opacity power of all the pigments used in papermaking. However, it costs 5 to 10 times more than other commonly used fillers. It is mainly used in paper with low basis weights that have demanding requirements for opacity.

Titanium is the fourth most abundant chemical element on earth and occurs in the form of oxides or mixed oxides of other elements. Titanium dioxide is produced by the sulfate or the chloride process, and it has three modifications with different structures, giving therefore

different physical properties. They are rutile, anatase, and brookite. But, due to their thermodynamic characteristics and physical properties, rutile and anatase are the most important in the field. These pigments show an extremely high refractive index (2.75 for rutile and 2.55 for anatase), even when the paper is wet (*eg*. label paper). Rutile is used in grades that require high opacity, while anatase supports OBAs better. However, the size of the particles of titanium dioxide are extremely small with sizes between 0.2μm and 0.25μm, and this mineral has a very complex chemistry in application, causing difficulties of retention is the paper web (Holik, 2013; Morsy *et al.*, 2015; Hubbe and Gill, 2016).

As paper coating, TiO_2 is the most effective white pigment and provides the increase of opacity of the coated paper, and it also enhances the topographical properties of the paper surface. The quality improvements, besides the ones already mentioned, are related to the smoothness and, most importantly, the printability and print image quality. These pigments are often used together with extenders to provide highest efficiency (Holik, 2013; Morsy *et al.*, 2015).

2.4.4   Ground Calcium Carbonate

Natural calcium carbonate, $CaCO_3$, commonly known as GCC, is a filler with an extreme importance in the industry. It is predominantly applied in woodfree uncoated papers, mechanical uncoated paper, newsprint, and coating base papers. The mineral form of GCC occurs in limestones, chalks or marbles. Depending on the ambient pressure, temperature and water contact, calcium carbonate has six different polymorphs: amorphous calcium carbonate (ACC), calcium carbonate hexahydratate, calcium carbonate monohydratate, vaterite, aragonite and calcite; its thermodynamic stability increases from ACC to calcite (Hu, Shao, Cai, *et al.*, 2009; El-Sheikh *et al.*, 2013; Hubbe and Gill, 2016; Jimoh, Okoye, *et al.*, 2017).

The crystal structure of GCC is rhombohedral, and fillers based on limestone and marble are chosen in the papermaking industry to give higher brightness. In the production of newsprint, where there is less demand for brightness, fillers based on chalk are used because of its lower brightness. The finesses of GCC fillers for paper gives higher gloss and may improve brightness, thanks to higher light scattering, low abrasiveness, and low dusting out of the paper surface in the printing process. Coarser GCC particles, at a given percentage, tend to increase the strength of the sheet and requires low demand of sizing agents, when compared with other types of fillers.

Another advantage in the use of GCC in the papermaking is its low cost. The use of GCC also promotes drainage, reducing the energy of the drying stage of the papermaking process.

The negative surface charge of many GCC products can be controlled with the use of dispersants, otherwise the behaviour as wet-end additives can be affected.

Since calcium carbonate is soluble under acidic conditions, the papermaking environment must be near neutral or at slightly alkaline pH. Paper containing GCC produced under acidic conditions can decompose relatively faster, requiring expensive measures of conservation.

As coating pigment, GCC needs less amount of binders and allows drying energy savings. Its structural shape promotes excellent runnability even with high solid content and highest coating speed (Holik, 2013; Bajpai, 2015).

Nowadays, GCC particles have been modified, originating a pigment with completely different morphologies and properties. The specific surface of this mineral can be increased and can provide excellent paper properties, such as good printability in offset and rotogravure and easy gloss development (Wang *et al.*, 2009).

2.4.5 Precipitated Calcium Carbonate

Starting from GCC particles, it is possible to synthesize another type of $CaCO_3$, by a precipitation reaction, called precipitated calcium carbonate (PCC). The new mineral has different morphologies, characteristics and crystal size from the precursor material. Generally, GCC is cheaper than PCC, although due to the grinding process that is necessary to form particles size of GCC with several microns, its price increases due to the high-energy costs involved (Hu, Shao, Cai, *et al.*, 2009).

PCC has several advantages over GCC because of its unique properties, high purity, and a uniform particle size distribution and shape. The shape, sizes and properties of the crystal surface, depends on the specific synthesis reaction process used. Usually, commercial PCC purity is about 97% on $CaCO_3$ content, and the remainder is $MgCO_3$ and other residues of the industrial process (Hu, Shao, Cai, *et al.*, 2009; El-Sheikh *et al.*, 2013; Holik, 2013; Bajpai, 2015; Jimoh, Okoye, *et al.*, 2017).

There are several methods of producing PCC, where the simplest one is a solid-liquid route, which involves a direct reaction in aqueous solution between the ions Ca^{2+} and CO_3^{-2}. Other common route is the carbonation method, a solid-liquid-gas reaction. Although it is a slower method compared with the first one, it is the procedure most used by the industries due to its low cost, higher yield and higher purity. Depending on the geochemical composition, the

original rock, rich in carbonate, is calcined using temperatures from 900 to 1000 ºC to produce calcium oxide (also called lime) and carbon dioxide. In this step, 44% of the mineral's original mass is lost. After this, the calcium oxide is treated with distilled water to produce calcium hydroxide (milk of lime). The resulting material is then purified and carbonated with the carbon dioxide (CO_2) obtained earlier in the calcination process. These steps are shown below in the Reactions 2.1, 2.2 and 2.3. The low solubility that CO_2 has in water leads to a slower reaction (Geyssant, 2003; Xiang *et al.*, 2004; Bajpai, 2015; Hubbe and Gill, 2016; Jimoh, Okoye, *et al.*, 2017).

Calcination of the limestone:
$$CaCO_3 \rightarrow CaO + CO_2 \tag{2.1}$$

Calcium hydroxide production:
$$CaO + H_2O \rightarrow Ca(OH)_2 \tag{2.2}$$

Precipitation:
$$Ca(OH)_2 + CO_2 \rightarrow CaCO_3 (\downarrow) + H_2O \tag{2.3}$$
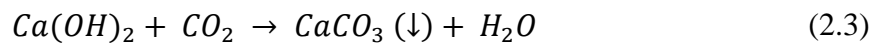
During the precipitation step, the exposure of $Ca(OH)_2$ to CO_2 gradually lowers the pH. This is one of the factors that may influence the size and morphology of the product crystal. Other factors include temperature, agitation, pressure, reaction speed, addition of other soluble materials. The PCC particles have a more uniform structure compared with GCC. The end material can have several structures such as scalenohedral, rhombohedral and acicular, as represented in Figure 5.
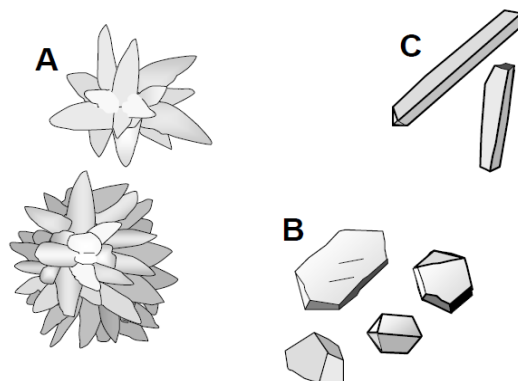
Figure 5. Different morphologies of PCC. A – Scalenohedral (rosette-shaped), B – Rhombohedral (cubic-shaped), C - Acicular (needle-shaped). From Hubbe and Gill (2016)

PCC is the most widely used filler for paper and this is motivated by its high light scattering, making possible to achieve great results of opacity and brightness without the use of expensive minerals, such as TiO_2 (Velho, 2003).

The most common kind of PCC used is the scalenohedral one. This shape gives paper favourable properties such as stiffness and bulk, when compared with other fillers. Although, a higher bulk decreases the strength properties because the sheet becomes more porous and permeable (Bajpai, 2015; Hubbe and Gill, 2016). This property is also propitious to ink receptivity, resulting in better print quality.

As coating pigment, when blended with GCC, it is possible to adjust a balance between bulking properties and strength and runnability (Laufamann *et al.*, 2000). Also, strength of the paper can also be enhanced when using a suspension of PCC with cooking starch.

PCC is a mineral that is in constant study as there are numerous factors that can contribute to its modification and to improve its use in a specific area. For this reason, there are some companies specialized in the polymorphism's study of this material for paper application and improvement of its properties, when used as filler or coating pigment (Omya, 2015; Imerys, 2017; Inc., 2017).

Some researchers reported the use of modified PCC as paper filler to improve its properties. Loading material of PCC with whiskers shape may confer improvements of electric resistance and elasticity modulus (Cheng *et al.*, 2004; Chen, Qian and An, 2011). Also, Hu *et al.* (2009) showed improvements of the physical and optical properties of the paper when fillers of needle-shape aragonite were used.

To better understand how the modification of PCC occurs is the main study of this thesis; thus, it is important to make a review (Section 2.5) of the research that was already made to obtain neddle-shape, whisker or lamellar structure. Other aspect to have in consideration is the use of the organic additives as CIT and/or sodium citrate (SC) with calcium carbonate to obtain the mentioned structures.

2.5   Calcium carbonate and Organic Compounds

In the previous work, one of the techniques used to deconstruct the cellulosic matrix of the paper, to obtain its mineral loading without its degradation, was an enzymatic complex. This complex is activated with the use of SC buffer. This led to a white dust as residue that was after characterized by several methods in which is included FESEM. The obtained pictures show a completely different morphology of the original PCC used as loading filler. The residue

obtained has lamellar morphology. Thus, it was possible to conclude that the used buffer causes the change on the shape of PCC (Carecho, 2016).

To better understand how the PCC is influenced by the citrate, it is important to have an idea of the approaches already tested (with citrate or other organic compounds) to obtain the same or similar structures, such as needle-shape or other elongated shapes. The application of this modified particles on paper is also a point to take into account. Other aspect to have in consideration is the use of citrate with calcium carbonate and in which aspects it influences this mineral.

2.5.1   A review

The controlled synthesis of calcium carbonate has received much attention due to its wide application in many industrial fields, including paper, paint, and plastics production (Geyssant, 2003). As it was said in the previous sections, there are several aspects that can be manipulated to control the morphology and the properties of the end particles. Numerous researches are being made to study the behaviour of this particular mineral, and some of them will be presented below. A resume of these studies can be found in Table 3.

Meldrum and Hyde (2001) synthesized calcium carbonate precipitated from saturated solutions in the presence of magnesium (Mg) and organic additives (citric and malic acid (MA), both known to enhance incorporation of Mg in the calcite lattice). Their aim was to investigate the impact in the end particles morphologies mingling Mg with the calcite. The particles precipitation was made by the carbonation process, at pH 7 at room temperature and pressure, and the crystals were grown for ten weeks. The resulted material exhibited a range of shapes of calcite and some of them can be pointed out:

-   Precipitation in the absence of Mg (only using calcium carbonate and the organic acids): the influence of malic and citric acids was very striking. CIT showed a more pronounced affect in the crystal morphology and growth then the malic acid, while malic acid exerted influence on crystal morphology even at very low concentrations. The final result showed elongated crystals with both acids, depending on the concentration used.

-   Precipitation in the presence of Mg and organic acids: from this experiment resulted even more pronounced structural modifications, and once again, CIT exerted a stronger

morphological influence. Depending on the concentrations used, it can be highlighted the appearance of elongated and lamellar crystals.

Table 3. Studies of PCC modified morphology

Additives	Parameters	Morphology	Synthesis Process	References
CIT MA	pH=7 Ambient temperature and pressure	Elongated Lamellar	Carbonation	Meldrum and Hyde (2001)
EDTA CIT	50˚C pH = 9-11	Needle-like Rhombohedral	Solution	Westin and Rasmuson (2003)
PAA PEG PVA CTAB	25 - 80˚C pH = 10	Elipsoidal Wiskers Dendritic	Solution	Yu *et al.* (2004)
CTBA EDTA PDDA	30 - 90˚C pH = 9	Rectangular Plate-like Branch-like Apple-core shape	Solution	Altay, Shahwan and Tanoğlu (2007)
CIT MA	80˚C Controlled pH	Needle-like	Carbonation	Park *et al.* (2008)
SS	60 ºC	Lamellar	Solution	Wang *et al* (2009)
None	30 - 80˚C	Lamellar Rod-like	Solution	Chen and Xiang (2009)
None	70˚C	Needle-like	Solution	Hu, Shao, Cai, *et al.*, (2009)

Westin and Rasmuson (2003) investigated the influence of ethylenediaminetetraacetic acid (EDTA) and citrate on the process of precipitation of calcium carbonate. The effect of the concentration of this organic compounds on the particle size and shape was also observed. Other process conditions were also studied such as feed rate, calcium/carbonate ratio and pH. The reaction temperature was maintained at 50ºC and the pH varied from 9 to 11. The resulted

obtained particles presented changes in their morphology depending on the absence or use of additives. Without the presence of additives, the obtained material was needle-like shaped. The complexing agents proved to have strong influence on the crystals' morphology: CIT promotes the rhombic structure at pH 10 and a calcium/carbonate ratio of ¼, whereas the presence of EDTA generates mostly spherical particles.

Cheng *et al.* (2004) studied the crystallization of $CaCO_3$ particles in the absence and presence of polyacrylic acid (PAA), polyethylene glycol (PEG) and polyvinyl alcohol (PVA) and cetyltrimethylammonium bromide (CTAB), by a solution process. The reaction occurred at temperatures of 25ºC and 80ºC, respectively, and pH 10. The resultant solution was allowed to stand under static conditions for 24h. The reference particles (without any additive) revealed to be a plate-like aggregate of calcite at 25ºC, and rhombohedral at 80ºC. This study showed that PAA has significant influence on the morphology of $CaCO_3$ at 25ºC, forming ellipsoidal particles. Also, with the use of CTAB at 80ºC, there were obtained aragonite wiskers. PVA induced also great modification at 80ºC, forming drendrite-shaped aggregates. PEG showed no influence in crystal modification.

Altay, Shahwan and Tanoğlu (2007) investigated the influence of the additives CTAB, EDTA and polydiallyldimethylammonium chloride (PDDA) on the morphology of $CaCO_3$ at variable temperature (30ºC, 50ºC, 70ºC, and 90ºC). The precipitation reaction was made by a solution process, at pH 9 and with an aging time of 24h. The effects of these additives were studied, showing that the higher temperature has great influence on the particles' modification. PDDA additive transforms the original rhombohedral shape into rectangular prism calcite. The CTAB at lower temperatures forms plate-like crystals, while at higher temperatures promotes the formation of branch-like particles. When adding EDTA to the solution, the crystals obtained are composed by calcite and aragonite and the final morphology at lower temperature is similar to an apple core; however with the increase of the temperature, the crystal tends to elongate and at 90ºC the particle shape is prismatic rod.

Park *et al.* (2008) investigated the effects of the ions Mg^{2+} and organic additives such as citric and malic acid in the synthesis of PCC by the carbonation process. The reaction occurred at 80ºC and controlled pH, and the obtained crystals were filtered and dried for 12h at 80ºC. The study showed that the crystals' aspect ratio increases as the concentration of Mg^{2+} increases; also there is an optimal ratio Mg/CIT where the growth of needle-like minerals are

favoured. Also, SEM images show needle-like shape well defined when citric or malic acid are used. The authors also consider that these organic additives may disrupt aragonite formation by reaction with magnesium ions rather than facilitating calcium carbonate synthesis through association with calcium ions.

Wang *et al.* (2009) obtained lamellar aragonite by using sodium stearate (SS) as additive in the solution process of precipitation of $CaCO_3$. The reaction occurred at 60 ºC for 15h. After this time, the precipitate was washed and dried for one day at 80 ºC. This additive was proven to not only modify the morphology of the precipitated aragonite, but also to increase its hydrophobicity.

Chen and Xiang (2009) synthesized $CaCO_3$ polymorphs with double injection of $CaCl_2$ and NH_4HCO_3 solutions without any additive. The temperatures used in this study vary from 30ºC to 80ºC. The resulted material was dried at 105ºC for 12h. The study of the influence of the temperature on the shape of the particles revealed that at 30ºC mushroom-like lamellar aggregates are formed, and with the increasing of the temperature the material's shape tends to be more lamellar; at 80ºC rod-like products were obtained. It was also noticed that the values of $[CO_3^{-2}]/[Ca^{+2}]$ decreased with the increase of temperature, and the authors say that this fact could be one of the reasons for the difference between the shapes formed at 30-40ºC and at 80ºC.

Hu *et al.* (2009) reported the synthesis of needle-like aragonite directly from GCC using a reversible reaction between magnesium chloride ($MgCl_2$) aqueous solution and GCC. The calcination process was not used in this case. The reaction occurs at the synthesis temperature of aragonite, 70ºC. The crystals were aged at room temperature for 2h.

The same authors (Hu *et al.*, 2009) introduced these same particles as paper fillers to evaluate the strength of the paper. Their results showed improvements in some paper properties such as tensile strength and folding endurance, when compared with paper using commercial PCC. The stiffness of the sheets on the machine direction was increased. This experiment revealed that the price of the paper can be decreased even when the loading with needle-like aragonite is increased.

2.5.2 Citric acid/ sodium citrate influence on calcium carbonate

The influence of CIT and its salt on calcium carbonate particles is not yet fully understood. However, there are some characteristics such as its low toxicity that make CIT one of the organic acids most used widely. The reaction of organic acids with carbonate compounds is complex due to its reversibility and for being thermodynamically limited by the presence of reaction products (Chatelain, Silberberg and Schechter, 1976).

CIT has three carboxylic (COOH) and one hydroxyl (OH) groups, which have a great importance in its reactions. Figure 6 shows CIT and SC molecules, respectively.
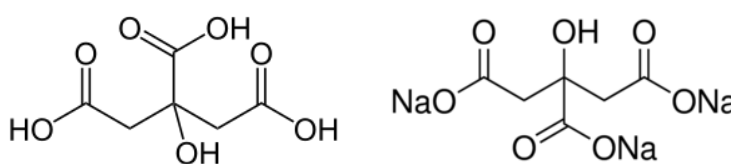

Figure 6. Citric Acid (left) and Sodium Citrate (right) molecules

In the presence of calcium ions, CIT behaves as a sequestering or as a chelation agent, resulting water-soluble or water-insoluble compounds, respectively. This depends on some factors such as the ionic strength, pH, and temperature of the mixture.

Some researchers had studied the behaviour of this carboxylic acid with calcium carbonate, mainly when used in the precipitation process (Reddy and Hoch, 2001; Wada, Kanamura and Umegaki, 2001; Westin and Rasmuson, 2003; Karar, Naamoune and Kahoul, 2016). One aspect in common in these studies is that CIT acts as a growth inhibitor during the crystallization step, and this phenomenon increases with the increasing of the concentration of CIT. Wada, Kanamura and Umegaki (2001) suggested that this inhibition capacity may be dependent on the carboxylic groups, by their adsorption onto the calcium carbonate particles. This mechanism may also contribute to the modification of the characteristic morphology of calcite crystals. The same study say that the bond between carboxylate ions (from the carboxylic acids) and free Ca^{2+} of the calcium carbonate surface, may lead to the increase of the particles hydrophobicity.

Karar, Naamoune and Kahoul (2016) also studied the effect of mixing CIT and SC with $CaCO_3$. As this mixture has two inhibitors, the chelation capacity for calcium ions is higher than the one with the two organic compounds used separately. This causes the increase of the nucleation time and the crystal size reduction. In this study, the formation of calcium citrate $(Ca_3(C_6H_5O_7)_2 \cdot 4H_2O)$ is also described. The deprotonation of CIT in the presence of SC chelate with Ca^{2+} forms a calcium-CIT complex, Figure 7.
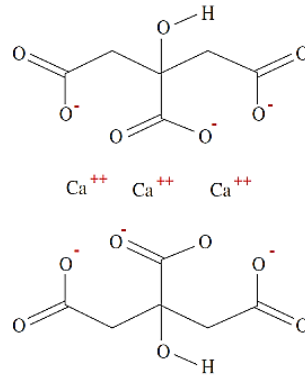
Figure 7. Calcium-Citric Acid complex. From Karar, Naamoune and Kahoul (2016)

CIT is a weak acid, it ionizes as the following steps (Reactions 2.4 to 2.7), and considering A = ($C_6H_4O_6$) (Gerardo, George and Marten, 2004; Apelblat, 2015; Karar, Naamoune and Kahoul, 2016).

$$H_3AOH \leftrightharpoons H_2AOH^- + H^+ \tag{2.4}$$

$$H_2AOH^- \leftrightharpoons HAOH^{2-} + H^+ \tag{2.5}$$

$$HAOH^{2-} \leftrightharpoons AOH^{3-} + H^+ \tag{2.6}$$

$$AOH^{3-} \leftrightharpoons AO^{4-} + H^+ \tag{2.7}$$
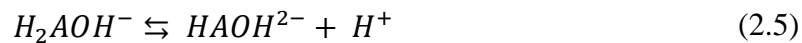
These reactions depend on the pH and the respective dissociation constant, pKa. At 25ºC, for CIT these values are pKa$_1$=3.13, pKa$_2$=4.76, pKa$_3$=6.4 and pKa$_4$=11.6 (Al-Khaldi *et al.*, 2007). The ionic distribution of CIT as function of pH is plotted in Figure 8 (Al-Khaldi *et al.*, 2003). This shows that when CIT is dissolved in water, its pH is in the range 1.7-2.1. With the increasing of pH, the carboxylic groups are released from the molecule, being free to accept the calcium ions in the solution, as concluded by Karar, Naamoune and Kahoul (2016).

Thus, as the pH value increases, more CIT (H_3AOH), di-hydrogen (H_2AOH^-), and mono-hydrogen ($HAOH^{2-}$) citrate ions are ionized to produce citrate ions (AOH^{3-}) at pH greater than 6.

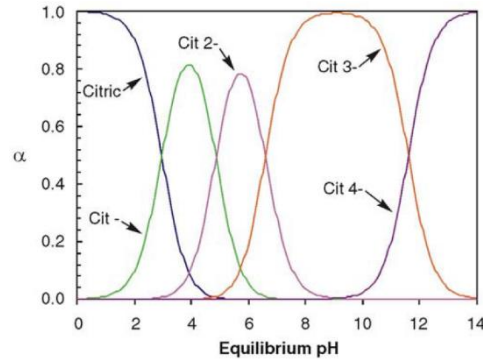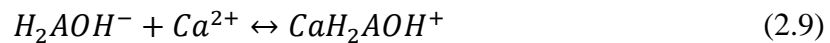Figure 8. Ionic distribution of citric acid as function of pH. From Al-Khaldi *et al.* (2003)

As CIT enters in contact with $CaCO_3$, calcium ions are released, as well as water and carbon dioxide (Reaction 2.8). Then the di-hydrogen citrate ions capture the calcium ions and form a calcium-CIT complex (Reaction 2.9)) (Al-Khaldi *et al.*, 2007).

$$2H^+ + CaCO_3 \leftrightarrow Ca^{2+} + H_2O + CO_2 \uparrow \qquad (2.8)$$

$$H_2AOH^- + Ca^{2+} \leftrightarrow CaH_2AOH^+ \qquad (2.9)$$
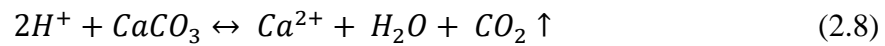
If the solubility limit of calcium citrate is exceeded, at pH $\geq$ 6 it precipitates, as described by the Reaction 2.10. In fact, (Carecho, 2016) reported that at this point of the reaction, the white suspension of PCC with SC turned transparent, turning white again after a few minutes - corresponding to the dissolution and posterior precipitation of calcium citrate.

$$Ca^{2+} + 2(CaH_2AOH^+)_{(aq)} \leftrightarrow Ca_3(AOH)_{2\ (s)} \downarrow\ + 4H^+ \qquad (2.10)$$
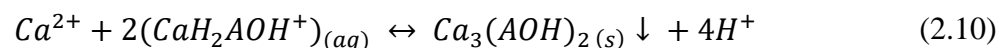
The formed calcium complex is insoluble in water and its solubility is not strongly dependent of the temperature, since as the temperature increases the solubility value is slightly increased (Apelblat, 1993).

Since the calcium citrate precipitation depends on the pH value, the presence of CO_2 is an important factor: CO_2 dissolves in water, forming carbonic acid (H_2CO_3) which reacts with $CaCO_3$ (Reaction 2.11 and 2.12).

$$CO_{2\,(g)} + H_2O \leftrightarrow H_2CO_{3\,(aq)} \qquad (2.11)$$

$$CaCO_3 + H_2CO_{3\,(aq)} \leftrightarrow 2\,HCO_{3\,(aq)}^- + Ca_{(aq)}^{2+} \qquad (2.12)$$
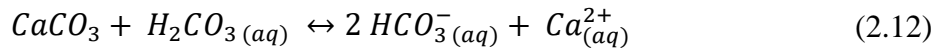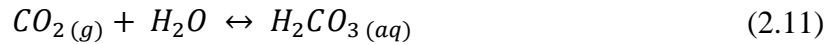
The previous reactions prevail at pH higher than 5, where the partial pressure of carbon dioxide exceeds the atmospheric pressure (Al-Khaldi *et al.*, 2007).

To sum up, the overall reaction between CIT and $CaCO_3$ can be written as presented in Reaction 2.13.

$$2\,C_6H_8O_7 + 3\,CaCO_3 \rightarrow Ca_3(C_6H_5O_7)_2 + 3\,CO_2 \uparrow + 3\,H_2O \qquad (2.13)$$

As the 2nd proton of CIT is being released, CO_2 is being formed allowing the formation of carbonic acid with the reaction with water. The di-hydrogen citrate ions accept the free calcium ions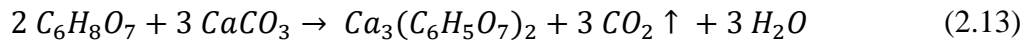, forming a calcium-CIT complex. The formation of carbonic acid seems to prevent the 3rd citric acid proton from spending. Since the 1st proton of carbonic acid has a pKa of 6.35, and the 3rd proton of CIT has a pKa of 6.4, the system is buffered around these pH values, due to the protons' competition. As the CIT concentration increases, the pH lowers, and its protons have a dominant effect. Thus, the release of the 3rd proton is promoted, and consequently the molecule can accept the calcium ions, forming the calcium citrate molecule (Al-Khaldi *et al.*, 2007 and Al-Khaldi *et al.*, 2003).

However, in none of these investigations is referred the formation of lamellar structures due to the reaction of calcium carbonate with CIT or SC. A more detailed study must be made to understand how the lamellar particles are originated in the presence of SC.

3   Materials and Methods

The aim of this dissertation, as previously referred, is to study the modifications on the scalenohedral PCC morphology when it is in contact with citrate buffer. The final mineral has a lamellar shape, and it is not yet understood the mechanism that originates this kind of structure. Thus, as starting point, the experimental protocol used in the complementary study made by Carecho (2016) was reproduced, and used as reference (Appendix A. I). After this, some process modifications were made in order to optimize the logistic of the reaction and reduce its time as well. To assess how the reaction conditions can enhance the formation of lamellar particles, a pH study was made, maintaining the temperature that was initially used. The influence of the ratio of CIT/PCC was also investigated.

The next step concerns the characterization of the obtained particles and posteriorly their application as coating pigment. The printing quality of the coated paper was evaluated. The behaviour of these particles used as paper filler with a content of 30% was also studied by the determination of paper properties.

3.1   PCC modification with sodium citrate buffer

This procedure is fairly simple and the reaction preparation starts by adding PCC (2 g) and ultrapure water (50 mL) in a 400 mL beaker. After, the mixture undergoes vigorous magnetic stirring with gradual heating up to 50 ℃. The citrate buffer 1M and pH 4.5 (preparation process in Appendix A. II.) is added until the reaction pH reaches 5.5, measured at 50 ℃. The addition of the buffer must be done slowly and the amount needed is about 40 mL (~ 8.4 g of CIT).

When the reaction conditions are reached, the mixture remains under stirring for 1h. After this time, the mixture is poured into falcon tubes to proceed the centrifugation step in the *Hettich Universal 32* equipment. The centrifugation must be done for 20 minutes and at 4500 rpm. This process should be repeated three times with two intermediated washes with distillate water.

The obtained solid residue is after dried in the oven (*Scientific series 9000*) at 40 ℃ until it is completely dry. Usually the drying stage requires one day, and to be more efficient the residue can be transferred to petri dishes, however some material may be lost. After, the dried material is grinded into a uniform dust and stored in a suitable recipient.

The industrial PCC used was provided by the research center RAIZ, and the reactants used were NaOH in pellets and CIT monohydrate.

3.1.1 pH and Ratio CIT/PCC study

To investigate the origin of the lamellar morphology with the use of SC buffer, some variables were changed from the reference procedure. Thus, there were four points in study:

- The influence of the buffer's pH and consequently the pH of the obtained suspension;
- The CIT/PCC ratio;
- The use of CIT in the absence of NaOH;
- The use of GCC instead of the PCC in the original procedure.

In order to have a better control of the CIT/PCC ratio, new protocols were created:

- A solution of CIT (1M) were prepared and poured drop-to-drop into the PCC suspension. When the reaction conditions are reached the pH is measured at 50 ºC (Appendix A. IV);
- Two different solutions were prepared, CIT 1M and NaOH 1M, and then poured separately drop-by-drop into the PCC suspension, until the pretended ratio/pH is reached. After, the pH of the final suspension is measured at 50ºC. A detailed description of this procedure can be found in Appendix A. V.

Therefore, the three procedures can be identified as:

a) SC 1M added to the PCC suspension and obtained in two different ways:

    a.1) by using a solution of NaOH 0.1 M until a pH of 4.5

    a.2) by using pellets of NaOH until the required pH was reached

b) Addition of CIT (1M)

c) Addition of CIT (1M) and NaOH (1M) to the PCC suspension.

Table 4 resumes the experiments that were made. The obtained particles were characterized posteriorly. For better understanding, the nomenclature of the obtained particles will be S (as sample) followed by its number, *eg*. S2.

Table 4. Experiments preformed to study the effect of sodium citrate and citric acid with PCC particles

Sample	Procedure	pH$_{buffer}$	pH$_{final}$ suspension	CIT/PCC	Appendix
0	Carecho, 2016	4.5	5.5	4.2	A. II.
1	a.1)	4.5	5.5	4.2	A. III.
2	a.2)	4.5	5.5	4.2	A. III.
3	a.2)	8	10.5	1.6	A. III.
4	b)	-	3	2	A. IV.
5	c)	-	8	2	A. V.
6	c)	-	5.5	2	A. V.
7	c)	-	5.5	4	A. V.
8	a.2)	4.5	8	2	A. III.
9	b)	-	5	1.5	A. IV.
10	b)	-	5.2	1.4	A. IV.
11	a.2)	6	8	4.2	A. III.
12	a.2) (GCC)	4.5	5.5	6.3	A. III.
13	b) (GCC)	-	7.5	1.4	A. IV.

After the reproduction of the reference protocol, the next objective was to test the influence of a citrate buffer with a high pH (S3). S4 was performing with the aim to test the influence of the absence of NaOH and lowering the CIT/PCC ratio, to produce a more economic compound.

S5, S6 and S7, followed the same protocol. Though, in S5 the suspension was kept at pH 8 to a ratio of CIT/PCC half of the reference, to test once again the influence of pH in the final suspension. S6 and S7 were made to evaluate the CIT/PCC ratio, maintaining the same pH as the reference.

To have a parallel with S5, the S8 experiment was made, where the starting protocol was the same as the reference.

S9 was tested to evaluate which amount of CIT was needed to reach the pH 5.5 to further evaluate if that amount was the needed to form lamellar morphology.

As in all the previous experiments the amount of citrate (or CIT) was in excess relatively to the amount of calcium carbonate, experiment 10 was made, in which stoichiometric amounts were used.

To have an approach of the CIT pKa, the citrate buffer of S11 was prepared in order to have a pH of 6, corresponding to the realising of the 2nd proton of the acid (as study in Section 2.5). The influence of other pKa were also tested in S3, and S4.

Finally, the starting material was changed to GCC. S12 follows the same protocol as S2, and S13 has the same procedure as S10.

3.1.2 Characterization of the obtained particles

The characterization step has the utmost importance since it can give a more detailed description about the particles that are being studied, and a comparison between the original and the modified particles can be made. For such purpose several techniques were used, such as Microscopy for particle visualization (size and shape), laser diffraction for particle size, Zeta Potential for surface charge and Thermogravimetric Analysis and Calcination for decomposition rates.

Optical Microscopy (OM)

The optical microscope is an instrument that, with the help of a system of lenses, allows the magnification of small samples using visible light. This equipment consists of mechanical component and an optical component. The mechanic part supports and controls the optical part, and the latter promotes the images' enlargement. This equipment can provide a first approach to the sample in study, giving an idea of its shape and size.

The microscope used in this characterization was the *Olympus BH2* and it was connected to a system with a camera (*Color View III)* and a digital programme (*Analysis 5*) through which the samples can be seen.

Only the particles that apparently had a lamellar shape were chosen to continue with the characterization process.

Field Emission Scanning Electron Microscopy (FESEM)

The principle of this technique is based on the emission of an electron beam, through magnetic lenses that bombards the surface of the dried conductive sample. As a result, secondary electrons are emitted from each point of the object and are captured by a detector. Thus, by the decoding of the energy emitted by the electrons, it is possible to reproduce virtual images of the sample's surface. With this method, it is possible to understand some characteristics of the material as its size, its morphology and its topography (Dedavid, Gomes and Machado, 2007; Alyamani and Lemine, 2012).

The tests were performed in the LED&MAT laboratory of the *Instituto Pedro Nunes* (IPN) and the equipment used was the *Zeiss Gemini 2 Merlin Compact/VP Compact, Field Emission Scanning Electron Microscopy*. The samples were placed into a carbon tape and identified. In this analysis the samples were not coated with gold, as it would normally be done.

The aim of the coating is to help the conduction of the electrons and hence making possible to achieve an image with better resolution. There were obtained pictures with magnifications of 20000x, 7500x and 3500x. To improve the sharpness and the definition of the obtained image, it was introduced an inert gas above the sample during its collection.

With this analysis it was possible to confirm the real shape of the particles in study and only the particles with lamellar morphology were chosen to continue with the characterization stage.

Calcination at 900 ºC

The calcination at 900 ºC has the aim of decomposing the inorganic material present in the samples, causing the degradation of $CaCO_3$ into CaO, as described in Reaction 3.1.

$$CaCO_3 \rightarrow CaO + CO_2 \tag{3.1}$$

This technique was used to chemically characterize the samples, since its composition is still unknown. The original PCC and the modified particles were placed in the oven until it reaches 525 ºC to make sure that all the organics were decomposed. The weight was registered and the particles were placed once again in the oven for 14h up to 900 ºC. The protocol used followed the standard TAPPI 413.

Thermogravimetric analysis/differential scanning calorimetry (TGA/DSC)

This analysis allows the evaluation of the thermal stability of a sample and the amount of organic and inorganic parts present on it. The principle of TGA is related the weight changes in a sample as function of the temperature and time in a controlled atmosphere and the obtained results gives an idea of the material composition. The DSC is based on the measurement of the heat flow rate from a sample to obtain thermal critical points of the substances (Linseis, 2012a, 2012b). The equipment used was a *TA Instruments SDTQ600*, and approximately 10g of each sample were added to the pan and submitted to a 10 ºC/min heating rate, from room temperature to 900 ºC.

Laser Diffraction Spectrometry (LDS)

The aim of this technique is to measure the particle size distribution of the sample. The operation method consists in passing the particles through a focus laser beam. The light is scattered by the dispersed particles at an angle that is inversely proportional to their size and photosensitive detectors measure its angular intensity. Knowing the material's refraction index and the dispersing medium, it is possible to convert the diffraction pattern into the size distribution, with the Lorenz-Mie theory. However, even though the particles may present irregular shapes, the LDS considers that the particles have spherical shape, defining the results as equivalent spherical diameter.

For the LDS measurement, the sample needs to be previously prepared. For that, a suspension of 1wt% of the material is made, where about three drops of dispersing agent (ammonium polycarbonate 6 % (v/v), Targon® 1128) was added before adding the water. The suspension was subjected to magnetic stirring for 20 minutes and then placed in a sonication bath (50 kHz) for 15 minutes. After this time, the measurement can be done by adding a small volume of the suspension to a 700 mL of water in the equipment vessel until reaching an obscuration around 10 – 20%. The measurement was carried out under stirring (2000 rpm).

The analysis was done in the *Malvern Instruments' Mastersizer 2000* that allows the measurement of particle sizes between 0.02 and 2000 µm.

Electrophoretic Light Scattering (ELS)

The ELS allows the measurement of the surface charge of the particles in an aqueous medium. In this technique, the particles in suspension are subjected to an electric field that makes them move with a velocity related with their zeta potential (ζ). This value is a measure of the attraction-repulsion magnitude between the particles. A higher potential zeta represents a higher stability of the suspension. Charged particles repel themselves and this prevents the natural tendency of aggregation between particles.

The sample needs to be prepared before its analysis, with a similar protocol used in the LDS. However, the dispersant agent is not added and the suspension here is about 0.1 wt% to obtain results of good quality.

To perform this analysis, a *Malvern Instruments' Zetasizer Nano ZS* was used, and the zeta potential was evaluated at the environmental room temperature with an equilibrium time of 120 seconds.

3.2   Coating and Printing Quality

After the characterization, the modified PCC particles were applied as coating pigment over printing and writing paper produced from a bleached Kraft pulp from *Eucaliptus Globulus*, with a basis weight of 80 g/m^2 – namely paper base (PB). The coating properties and printing quality were evaluated in RAIZ.

3.2.1   Coating Process
The coating suspension is made with cationic starch (12 wt%) previously prepared (Appendix B. I.), the modified PCC particles, a few drops of dispersing agent and a small amount of water.

The suspension had the formulation described in Table 5.

Table 5. Formulation of the coating suspension

Additives	Quantity (g)
Starch suspension (12 wt%)	12.5
PCC	3
Dispersing agent (Targon $^®$)	0.25
Water	2 – 4 mL

To prepare the coating suspension, the PCC particles are inserted in a beaker, and then drops of dispersant are added. After, the water must be added drop-by-drop while the operator blends the mixture with a stirring rod until a paste is formed. This mixture should not be too fluid. The next step is the addition of the starch suspension. The final suspension must be stirred magnetically until a uniform mixture is obtained.

To perform the coating stage, 5 mL of the suspension are taken from the beaker with a plastic syringe and then poured along the applicator rod of the bench coating equipment. The coating equipment is a *Mathis SVA-IR-B*, which operates at different speeds of the applicator rod. The rod used was smooth with a diameter of 0.15 mm.

The drying process of the coated papers is divided in two stages: first, the IR-dryer dries the coating layer at the same time as it is done, and then the coated paper is exposed to the room air for some time.

The formulation and the process used are the same for the modified particles. There were made at least two duplicates for each type of particles. The coated papers were cut into an A4 sheet and the 'pick-up' was determined in RAIZ.

3.2.2 Coating Properties

After the 'pick-up' determination, two properties of the coated paper were evaluated: its air permeability and roughness. The air permeability was done by the Gurley's method (ISO 5636-5), in which the time that takes 100 mL of air flow to pass through the paper sheet is measured, using the *Gurley SE 121* equipment. The Bendsten method (ISO 8791-2) was used to measure the air flow that passes in between a circular head and the paper surface, giving in this way the roughness of the paper. This test was performed in the equipment *L&W Bendtsen*.

3.2.3 Printing Quality

To perform the printing quality analysis, a test mask (Figure 9) was printed in each of the coated paper. This was made with a *HP PhotoSmart B8850-IJTarget 13* in its best printing quality mode. To evaluate the quality parameters, the spectrophotometers *X-Rite i1* and *QEA PIASII* were used (Figure 9).

The optical density of the colours black, magenta, cyan, and yellow was measured with the *X-Rite i1* to determine the gamut area and volume. The print-through and show-through was also calculated with the help of this equipment.

The *QEA PIASII* was used to determine the line raggedness, the black and white feathering, and colour-to-colour bleed.
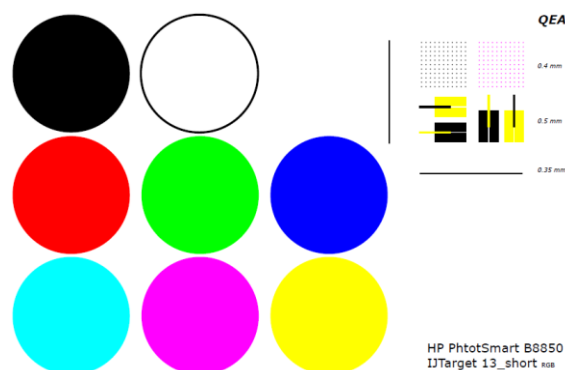

Figure 9. HP PhotoSmart printing quality test mask

3.2.4   Coating characterization

After the printing quality analysis, the coated papers with the highest values of gamut area were analysed by image analysis SEM (Scanning Electron Microscope). The resulting images from this technique result from a scan made by a beam of electron to the samples' surface. The electrons interact with the atoms of the sample, sending back signals with information of the topography of the sample.

The analysis was performed in University of Aveiro in the equipment *Hitachi (S4100)* at 15 kV, with double deposition of carbon.

3.3   Paper Testing

After the modification of the PCC particles and their characterization, besides the testing as coating pigment, they were also used as paper filler. For that, there were made handsheets and later their characterization. These procedures were performed in RAIZ, where it is available all the needed equipment.

3.3.1   Production of Handsheets

Before the sheets production, the first thing to do is to prepare the raw material and the additives needed to the production of P&W paper. The fiber used was previously refined in a conical refiner and having a Schopper-Riegle of 32.

In order to reduce the loss of additives during the paper formation, an aqueous solution of a retention agent (0.025 wt%) was used: cationic polyacrylamide (CPAM) with the commercial name Percol®. The sizing agent used was the alkenyl succinic anhydride (ASA) that was later added to a starch suspension 2.5% (wt%). Finally, an aqueous suspension (1 wt%) with the mineral loading was made. The procedures of these suspensions can be found in Appendix C. I – III.

The mixing of the enumerated compounds has to comply with the mixing times that are previously established. Those times can be found in Table 6 as well as the amount of fiber and additives needed to obtain a sheet with a weight of 1.6 g and a grammage of 80 g/m^2. To accomplish this task, an adequate equipment is needed, the batch handsheet former *MARVI (model 255/SA)*.

All the protocols related with the sheets formation, pressing and conditioning are described in Appendix D.

Table 6. Sheet formulation: Fibers, additives and contact times

Components	Quantities (g)	Adding time (min)
Fiber	1.102	0'
PCC	0.48	0'
Starch	0.016	2'
ASA	0.02	2'
CPAM	0.00032	4':30''

3.3.2 Handsheets Characterization

The paper characterization was made after its drying in the paper testing room. The room conditions follow the ISO 187 that establishes constant temperature and humidity, 23 ºC± 1 and 50% ± 2%, respectively.

First, non-destructive properties are evaluated, such as optical and mechanical properties. After, the sheets are cut following the standard ISO 5269/1, to proceed with the structural tests. Table 7 has a description of the equipment and its respective standard used to determine the optical, structural and mechanic properties of the handsheets.

Table 7. Paper testing properties: Equipment and Standards

	Property	Unit	Standard	Equipment
Optical	Opacity	%	ISO 2471	L&W Elrepho
	Brightness R457	%	ISO 2470	L&W Elrepho
	Light scattering coefficient	m^2/kg	ISO 9416	L&W Elrepho
Structural	Grammage	g/m^2	ISO 5270	Mettler HK 160
	Thickness	µm	ISO 534	Micrometer SE 051 D2
	Bulk	cm^3/g	EN 534	Calculated
	Permeability (Gurley)	s/100mL	ISO 5636-5	Gurley SE 121
	Roughness (Bendtsen)	mL/min	ISO 8791-2	L&W Bendtsen
Mechanical	Internal resistance	J/m^2	TAPPI 403	Scott Internal Bond Tester
	Tensile strength	kN/m	ISO 1924/2	Alwetron TH1
	Stiffness	kN/m	ISO 1924/3	Alwetron TH2
	Stretch	%	ISO 1924/4	Alwetron TH3
	Burst strength	kPa	ISO 2758	Burst-O-Matic
	Tearing Resistance	mN	EN 21974	Elmendorf 125

3.3.3 Filler retention

After the sheets formation, it is necessary to know the amount of effective filler that was present in the paper. For that, the formed sheets were calcined at 525 ℃, for16h as described in the standard TAPPI 211. During this procedure, the organic matter of a certain amount of paper is decomposed remaining at the end only the inorganics. After this determination, it was possible to calculate the filler that was retained in each sheet. This procedure was made in duplicate to each kind of sheets with different fillers.

4 Results and Discussion

In this section, the results obtained by the characterization techniques described in Chapter 3 will be analysed and discussed. The order of presentation will be the same as previously presented: first, an approach to the characterization of the original PCC and the modified particles will be made, and subsequently an evaluation of their effect as coating pigment and as paper filler.

4.1. Particles Characterization

The characterization of the original PCC and the modified particles was made in order to know their morphology, composition, size and surface charge.

4.1.1 Morphology

Optical Microscopy

The first attempting approach to analyse the morphology of the materials that were modified was made with the help of an optical microscope. Besides the low definition of the pictures, the particle's morphology can be noticed. In Table 8 are resumed the obtained morphologies for each reaction and the correspondent pictures can be found in Appendix E. I.

The sample obtained by Carecho (2016) will be taken as reference (S0, *Figure 10*) to evaluate the morphology of the particles posteriorly produced. Thus, it is possible to observed that lamellar shapes were obtained in the samples S1, S2 (*Figure 10*), S4, S9, S10, S11, S12, S13. However, the size of the particles is different from one another. S4, S9, S11, S13 presented a smaller dimension when compared with S0. The samples S6 and S7 present a higher aspect ratio and a morphology of what appears to be needle-type. S8 showed some lamellar particles, but it also had a high number of spherical particles. S3 and S5 showed to have spherical morphology.

The reactions of the particles presented in Figure 10 have the same protocol in terms of reaction conditions, although there were made some modifications in the process logistic. In S0 it was used mechanical stirring with the use of a blade agitator, while S2 undergo magnetic stirring. This can explain the broken aspect noticed in S0, compared with S2.
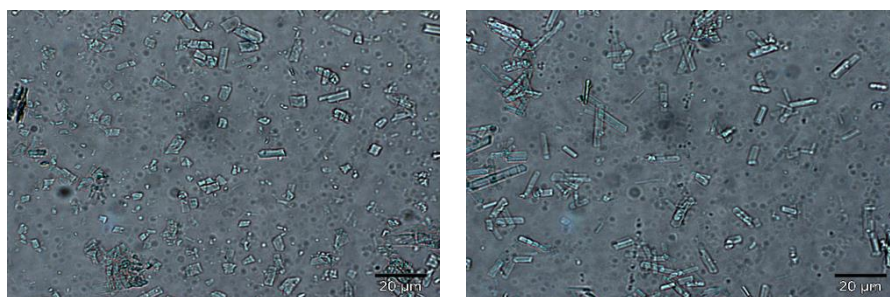
Figure 10. Reference particles, S0 (right) and its reproduced protocol, S2 (left). Magnification 50x.

Table 8. Morphology from the resulted samples observed by optical microscopy

Sample (S)	Procedure	pH$_{final}$ suspension	CIT/PCC	Morphology
0	Carecho, 2016	5.5	4.2	Lamellar
1	a.1)	5.5	4.2	Lamellar
2	a.2)	5.5	4.2	Lamellar
3	a.2)	10.5	1.6	Spherical
4	b)	3	2	Lamellar
5	c)	8	2	Spherical
6	c)	5.5	2	Needle – type
7	c)	5.5	4	Needle – type
8	a.2)	8	2	Lamellar and spherical
9	b)	5	1.5	Lamellar
10	b)	5.2	1.4	Lamellar
11	a.2)	8	4.2	Lamellar
12	a.2) (GCC)	5.5	6.3	Lamellar
13	b) (GCC)	7.5	1.4	Lamellar

The influence of the pH is very noticeable in this analysis. It can be pointed out that the CIT/PCC ratio is an important factor, since it influences the pH of the final suspension. Thus, this parameter is determinant in the formation of lamellar morphology. Suspensions with high pH (> 8) resulted in particles with spherical shape. The lamellar morphology is obtained at pH 5.5, and the CIT/PCC ratio can be adjusted depending on the protocol used.

In the absence of NaOH, particles with lamellar morphology are also formed but for CIT/PCC > 1.5 it is noticeable a high size reduction. This can indicate that the solution of CIT is degrading the particles of PCC.

To proceed with the characterization stage, the particles with spherical morphology were discarded, as well as lamellar particles with small size. Also, since S6 and S7 were performed with the same protocol and presented the same morphology, the one that had higher CIT/PCC ratio was also discarded.

Thus, the particles selected were S2 (reproduction of the reaction made by Carecho (2016)), S6 (from the new protocol but with lower CIT/PCC ratio and the same pH as S2), S10 (stoichiometric CIT/PCC ratio) and S12 (same protocol as S2 however, instead using PCC, GCC was used) and these were analysed by FESEM.

Reaction behaviour

To perform the coating and paper application there were produced more particles from the chosen samples. The yield of each reaction was calculated taking into account the amount of solids added in the beginning of the reactions and the obtained dried solid content. It can be found in Appendix E. II. The yield of the process varies mostly because of the centrifugation step, since in this stage there is high weight loss during the washing step.

With the new replicas of the reaction, it was noticed that the effective ratio of S12 is less the 6.3; the CIT/PCC ratio is in fact ca. 4. This means that the stirring must be vigorous to optimize the interaction between the reactants.

Carecho (2016) reported that when the SC is being added and the suspension reaches pH 6, there is a colour change of the mixture (from white to transparent), meaning its dissolution. After *ca*. 10 minutes the suspension precipitates and the original white colour appears. The same phenomenon was observed during these experimental procedures, but only when protocol a) was used, even when the starting material is GCC. However, since the lamellar morphology was originated with the other protocols, this phenomenon may not be an important factor to obtain the desired modification.

FESEM

To take a closer look on the particles morphology, the selected particles were subjected to FESEM analyses. To have a comparative image (Figure 11 a)), the research group provided to this work the SEM pictures of the original PCC. As it is possible to see, the original PCC used has a rosette morphology, characteristic of scalenohedral PCC. The modifications to this PCC resulted in lamellar particles, as expected. Figure 12 show the obtained modified particles S2, S6, S10 and S12 with magnification of 20 000x. The low definition of the pictures is due to the lack of particle coating with gold when the FESEM analysis was made.
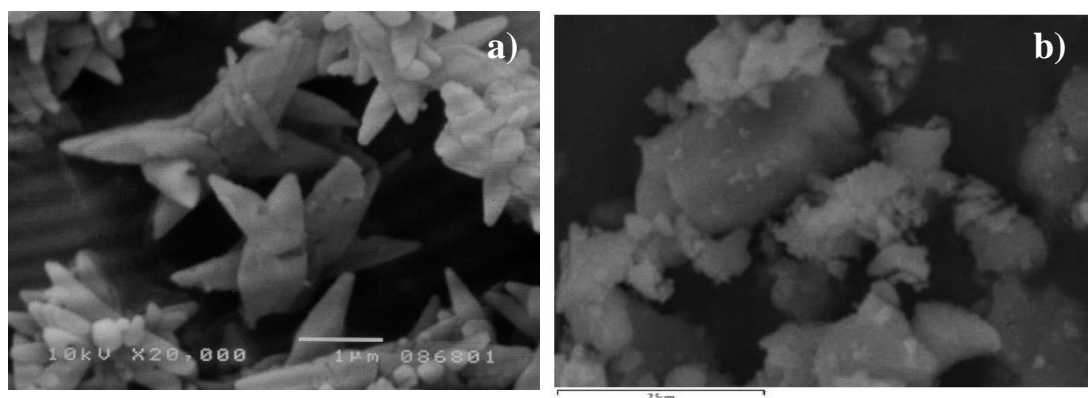

Figure 11. a) SEM image from the original PCC. Magnification 20k x. b) SEM image from the original GCC (H60). Magnification 20k x. Adapted from Sequeira (2014)

It is possible to observe the sharpness of lamellar particles S2 (a). S6 and S10 ((b) and c)) present also lamellar morphology although with higher aspect ratio.

The modified GCC (S12) can be compared with the SEM images (Figure 11 b)) of the GCC used by Sequeira (2014), the same starting material used in this work. The original GCC has a rhombohedral morphology and from the modification with the citrate buffer resulted particles with sharped edges, and a more platy structure.

Appendix E. III. contains images of the modified particles with other magnifications. There, it is revealed an unevenness of particle size distribution. Also, it can be seen that for S12, not all the particles presented sharp edges; some particles have rounded morphology similar to a coin. In the same appendix, the SEM images of S4 and S11 are also presented. The images confirm the lamellar morphology of S4, and it is notorious the low dimension of the particles, meaning that the action of CIT itself forms lamellar shapes but also disrupt them. On the other hand, S11 analysis show scalenohedral morphology, meaning that the optical microscopy analysis was not very accurate. These images reinforce the importance of the pH of the final suspension into the modification morphology – in a low pH lamellae are formed, but the aspect ratio of que particles is low; a high pH do not contribute to lamellae formation.
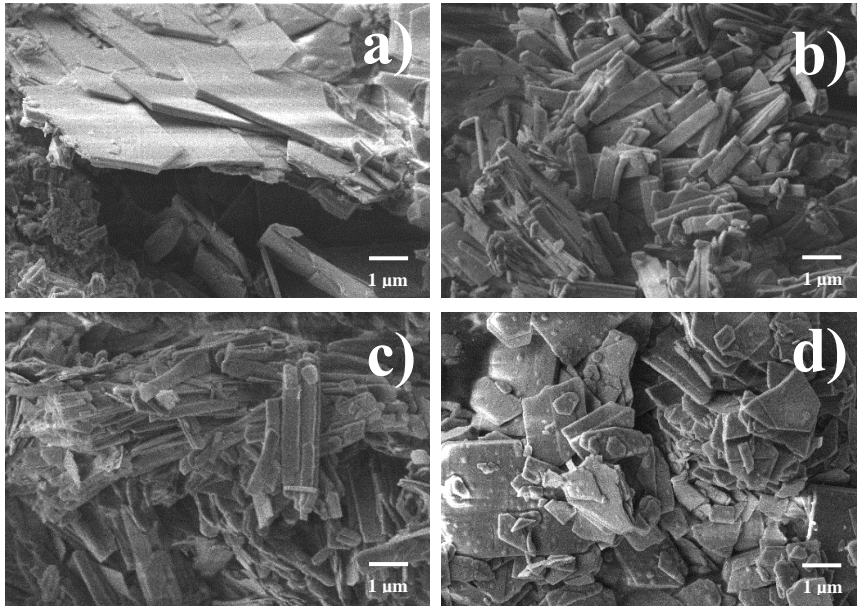
Figure 12. FESEM images of the modified particles. a) S2, b) S6, c) S10, d) S12; Magnification 20k x.

4.1.2 Thermogravimetric analysis

To better understand the chemical composition of the modified particles, the samples were investigated by thermogravimetric analysis.

The thermogram of the original PCC was provided by the research group and can be seen in Figure 13. The weight loss of the original PCC is about 43% (in the range of temperatures between 580 and 900 ℃) which corresponds to about 97 wt% of $CaCO_3$. The weight loss of *ca.* 3% is related to the impurities that the PCC may contain.

The TGA curves of the modified particles can be seen in Figure 14. The results presented are normalized, since the first approach revealed high percentage of water in the samples (Appendix F. IV). For this reason, the curves were changed in order to remove the highest percentage of water from the given weight loss values.
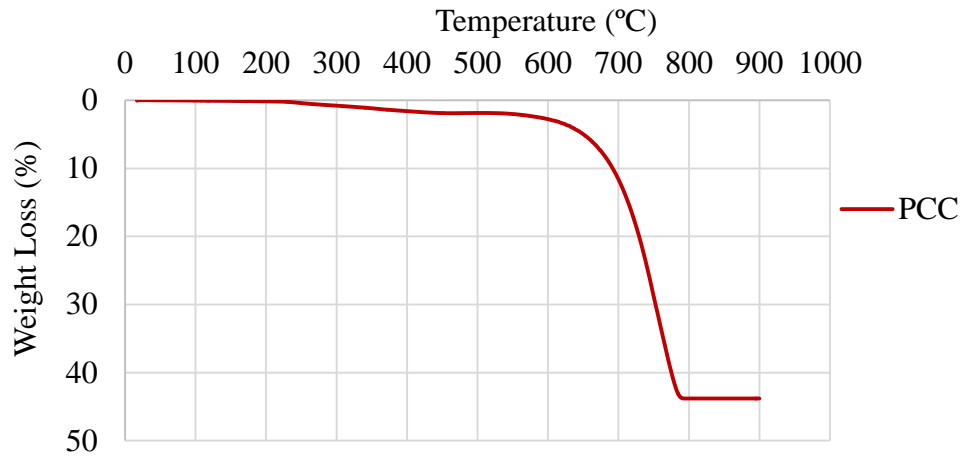
Figure 13. Thermogram of the original PCC

It is notorious that the thermograms of the modified particles are not similar to the one presented for the original PCC.

The complexity of the thermal behaviour of these particles can be noticed by the number of weight loss steps that exists from 105 ℃ to 900 ℃. In the literature review (Section 2.), it was described that some authors studied the reaction of calcium carbonate with citrate resulting $Ca_3(C_6H_5O_7)_2 \cdot 4H_2O$ as reaction product. The TGA curves of the modified particles are similar to those presented by Zhou *et al.* (1998) and Radfarnia and Iliuta (2013), suggesting that the resulted particles are actually composed by calcium citrate.
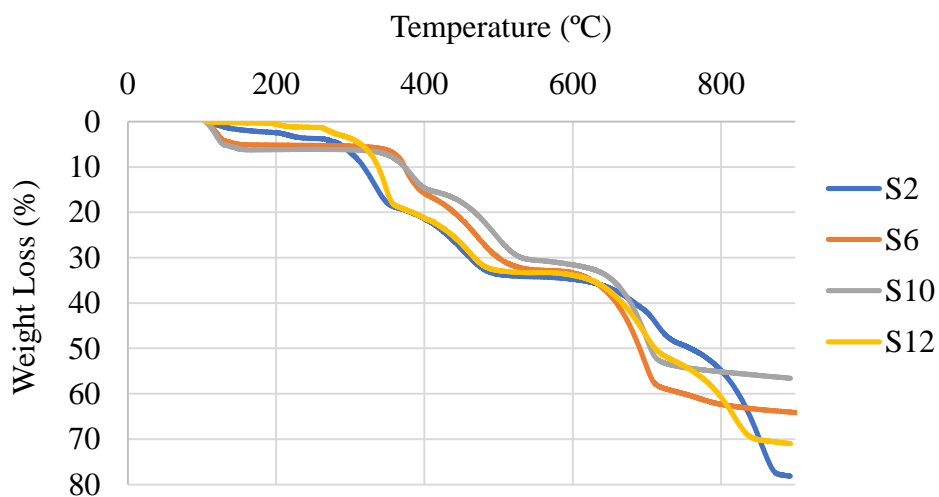

Figure 14. Thermograms of the modified particles

Mansour (1994) reported the reactions related to each step of the curve. Having in mind that some percentage of water was already released, the steps can be described as:

- Stage I, from 105ºC to 380 ºC: the steps of weight loss are related to the release of water molecules from $Ca_3(C_6H_5O_7)_2 \cdot 4H_2O$. It is also referred the melting of this compound at temperatures near 230 ºC.

$$Ca_3(C_6H_5O_7)_2 \cdot 4H_2O \rightarrow Ca_3(C_6H_5O_7)_2 \cdot 2H_2O \rightarrow Ca_3(C_6H_5O_7)_2 \qquad (4.1)$$
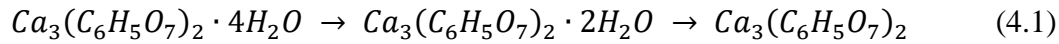
- Stage II, from 380 ºC to 570 ºC: decomposition of calcium citrate into intermediate compounds such as calcium aconitate $[Ca_3(C_6H_3O_6)_2]$ and $CaCO_3$, as well as some gases like CO and CH_4.

$$Ca_3(C_6H_5O_7)_2 \rightarrow \frac{1}{3}[Ca_3(C_6H_3O_6)_2] + 2\,CaCO_3 + 4\,CO + 2\,CH_4 \qquad (4.2)$$
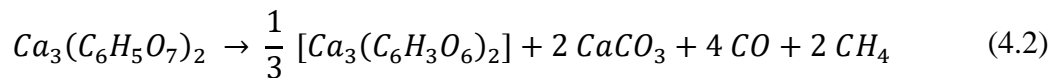
- Stage III, from 570 ºC to 800 ºC: the products of the previous reaction are decomposed into CaO, CO, H_2O and carbon compounds.

$$\frac{1}{3}[Ca_3(C_6H_3O_6)_2] + 2\,CaCO_3 + 4\,CO + 2\,CH_4 \rightarrow 3\,CaO + 6\,CO + H_2O + Other\ Compounds \qquad (4.3)$$
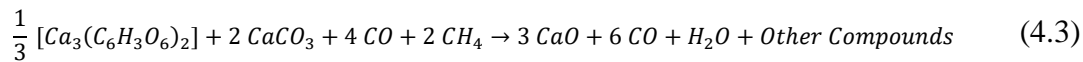
- Stage IV, temperatures higher than 800 ºC: all carbon produced is burned off.

Table 9 compiles the weight loss in each stage. It can be highlighted that, as its thermograms, S2 and S10, present similar behaviour.

Table 10 presents the amount of calcium citrate and $CaCO_3$ presented in the samples. The samples revealed to be in its majority composed by calcium citrate (65 – 52%), and ca. 24 – 38% of $CaCO_3$. Also there are some unidentified compounds contained in the samples. These values were obtained considering the weight used to measure the TGA and the stoichiometric coefficients presented in Reactions 4.1 – 4.3.

Table 9. Tonset, Tend and percentage of weight loss in each stage

	T_{onset}	T_{end}	Δ weight (%)	Stage
S2	63.92	348.8	21.35	I
	348.8	484.7	14.24	II
	484.7	668.1	14.11	III
	668.1	870.1	27.24	III and IV
S6	47.51	132.9	14.68	I
	132.9	384.9	11.04	I
	384.9	506.2	14.10	II
	506.2	711.9	27.62	III
S10	44.69	74.21	32.76	I
	74.21	397.4	6.690	I
	397.4	524.2	9.970	II
	524.2	713.9	16.90	III
S12	89.64	355.0	13.06	I
	354.98	485.9	11.67	II
	485.85	713.8	14.59	III
	713.78	836.4	13.23	III and IV

Table 10. Percentage of the different compounds in the modified particles

| Sample	% Calcium Citrate	%CaCO3	% Unidentified
2	61.5	24.7	13.8
6	52.7	37.9	9.40
10	64.4	25.9	9.70
12	65.0	26.0	9.00

4.1.3 Calcination

The calcination stage was made to quantify the inorganic material that exists in the samples. The reaction that occurs in this process is favoured by high temperatures. The particles were subjected to temperatures up to 900 ºC to make sure that all the calcium carbonate is decomposed in CaO and CO_2. This method is not very accurate, since the weight loss is determined by weighing after cooling in the desiccator, allowing a small percentage of the air humidity to be absorbed into the particles. For this reason, duplicates were made and then an average value was determined.

Table 11 shows the obtained percentage of weight presented in the temperature intervals in the calcination process and the percentage of $CaCO_3$ in the particles. However, this

percentage is not obtained in the same way for all particles. As said in Section 2, the performed reactions form a complex calcium-CIT, so it cannot be treated as pure $CaCO_3$. Mansour (1994) reported the decomposition of calcium citrate up to 900 ℃, and described several step decomposition reaction – also presented in the Section 4.1.2. Therefore, the percentage of $CaCO_3$ in the modified particles is calculated taking into account the reactions stoichiometric coefficients, as illustrated in Equation 4.1.:

$$Ca_3(C_6H_5O_7)_2 \xrightarrow[\Delta\ (105-525\ ℃)]{} 2\ CaCO_3 \xrightarrow[\Delta\ (525-900\ ℃)]{} 3\ CaO \qquad (4.4)$$
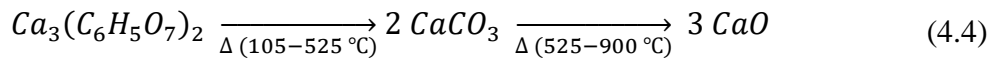
The degradation of $CaCO_3$ occurs from 570 ℃ to 800 ℃, so the calculations for the original PCC and the modified particles follow these equations:

- Original PCC:

$$\%\ (w/w)\ CaCO_3 = [weight\ loss\ (525\ ℃ - 900\ ℃)] \times \frac{100.1}{44} \qquad (4.1)$$

Where 100.1 g/mol is the molecular weight of $CaCO_3$ and 44 g/mol the molecular weight of CO_2.

- Modified Particles:

$$\%\ (w/w)\ CaCO_3 = [weight\ loss\ (525\ ℃ - 900\ ℃)] \times \frac{2 \times 100.1}{3 \times 56} \qquad (4.2)$$

Where 100.1 g/mol is the molecular weight of $CaCO_3$, 56 g/mol the molecular weight of CaO, and 2 and 3 the respective stoichiometric coefficients, as presented by the reactions 4.1 – 4.3.

It is possible to see that the modified particles lose more than half of its weight during this process. The major weight loss observed for these particles is in the interval of temperatures 105 ℃ – 525 ℃. These values correspond probably to the degradation of the calcium citrate and other compounds formed in each reaction. The modified samples only have about 38 – 22% of $CaCO_3$ in their composition (similar to those values obtained with the thermogravimetric analysis), meaning that the remain percentage corresponds to those same compounds. The amount of calcium citrate was not calculated using the same approach since the degradation of the complex at high temperatures is more complex than the one that happens in PCC.

Table 11. Modified Samples weight loss and percentage of CaCO$_3$

	% Weight			
Sample	**25 - 105 ºC**	**105 - 525 ºC**	**525 - 900 ºC**	**% CaCO3**
PCC	99.8	97.0	56.1	93.2
2	93.3	55.4	31.6	37.60
6	87.4	48.4	27.6	32.88
10	59.9	33.7	18.9	22.50
12	74.3	44.4	25.2	29.98

The original PCC only loses ca. 3% of its weight in the same range of temperatures, which can indicate the presence of impurities, probably due to its fabrication process (Gamelas, Lourenço and Ferreira, 2011).

4.1.4 Laser Diffraction Spectrometry

To know the size of the modified particles and compare it with the original PCC, the LDS technique was performed. This method is only used to make a comparison between particles, since the measurement in the equipment is given in terms of diameter, considering the particles as spheres. For each sample, two measurements were made and the values presented are an average of the obtained ones.

Figure 15 shows the size distribution of the particles in study. For S2, S6 and S10 (a), b) and c)), the comparison was made having into account the starting material used. For S12 (d), this comparison was not made since the starting material of this reaction was not characterized. However, in a future work this characterization should be made. For comparison between the modified and the original GCC, it will be taken as reference the result from Sequeira (2014).
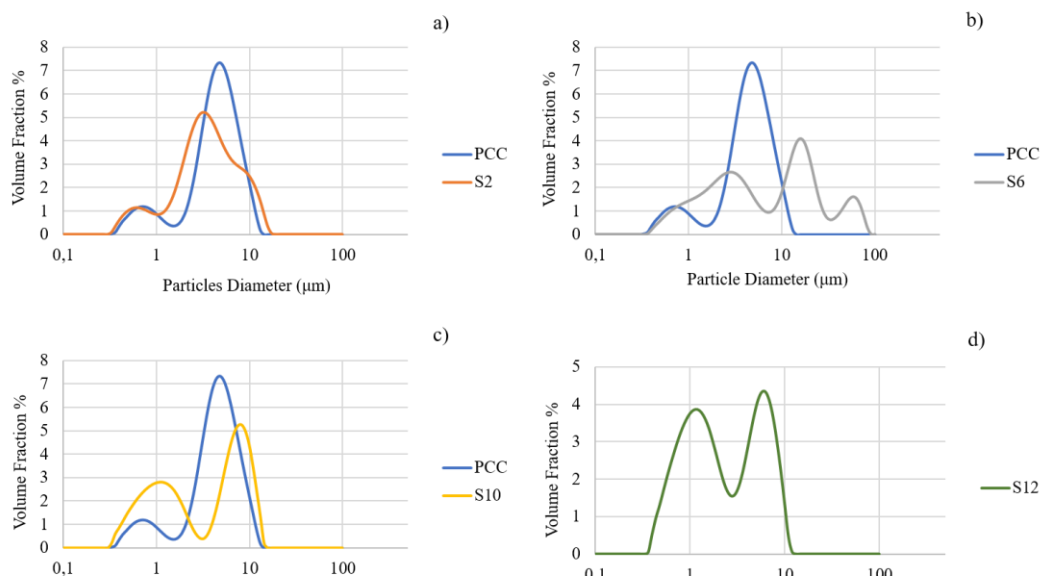

Figure 15. PCC and modified samples particle size distribution. a) S2, b) S6, c) S10 and d) S12.

The sized distribution of the PCC particles has a bimodal behaviour. Besides the use of a particles dispersant, stables aggregates are formed. Thus, the first peak corresponds to the range of sizes of the individual particles and the second one is related with the stable aggregates formed. The modified particles do not have the same kind of distribution as the PCC, with exception of S2, and the volume fraction needed for their analysis is less than the needed for PCC. It is possible to observe that the modified particles are smaller than the PCC.

The behaviour of S6 is not clear, as it has three distinct peaks, and the highest one corresponds to a majority of particles with diameter higher than 10 μm. S10 and S12 have two distinct peaks in the range of particles diameter of 1 μm and 10 μm. Sequeira (2014) reported that the original GCC has a unimodal distribution, which is different from the modified sample S12.

To better understand the dimension of the particles, Table 12 presents the range of the particle sizes in the different samples.

Table 12. Particles diameters

Sample	dp_{10} (μm)	dp_{50} (μm)	dp_{90} (μm)
PCC	0.96	4.30	7.83
S2	1.09	3.37	11.9
S6	0.98	6.36	55.8
S10	0.64	3.54	11.1
S12	0.95	3.77	12.0

As it was observed by the SEM images, S6 has particles with very different sizes. This is corroborated with the behaviour of the size distribution and, as it is possible to observe above, the sizes range from 0.98 to 55.8 μm. This can be justified with the experimental protocol used in this reaction: to lower the pH of the suspension, the PCC particles are first in contact with CIT (low pH) which promotes its deconstruction, and thus forming small particles sizes. As the pH stabilizes and the NaOH is added, this effect stops. The presence of the NaOH solution probably contributes to the elongation of these particles. Also the use of dispersant may not be sufficient to prevent the formation of aggregates with high dimensions, giving the size distribution a trimodal behaviour.

S10 is formed by the addition of CIT in stoichiometric ratio to the PCC (1.4). The same phenomena happen with regard to the deconstruction of the PCC, which justify the high peak the in fines zone.

The sample S12 is formed with GCC as starting material with the same protocol used in S2, and when these two samples are compared, it can be pointed out that there size is similar. Although, the peak of fines is higher for S12. The dp_{50} of the original GCC is about 2.1 µm (Sequeira, 2014), showing that the modification process increased its particle size.

During the measurement of S12, a high amount of the suspension was needed to reach the desired obscuration index. The suspension seemed to dissolve in the 700 mL of water used to perform the analysis. Further studies will be needed to understand the behaviour presented by these particles.

4.1.5 Electrophoretic Light Scattering

The zeta potential is important to analyse the electrostatic bonding between the particles. Table 13 presents the results obtained for each sample. To do this test, three measurements were performed with the same suspension and the presented values are an average.

Table 13. Zeta potential values

Sample	Zeta Potential (mV)
PCC	+ 8.57 ± 1.31
S2	- 22.8 ± 3.62
S6	- 18.7 ± 3.26
S10	- 16.2 ± 3.37
S12	- 40.5 ± 6.69

As it can be noticed, the zeta potential of the modified particles is negative. This can indicate that the suspensions have basic conditions. Values of zeta potential of calcium citrate cannot be found in the literature to use as comparative parameter. Though this superficial charge changes only happen for PCC. GCC particles have zeta potential of -29 mV (Sequeira, 2014) and its modified particles (S12) have -40 mV, revealing an increase of the particle stability. S2, S6 and S10 are located below the stability zone (that is in between ±30 and ±40, as reported by Chernyaev and Enberg (2015)), which may induce particle aggregation.

For filler application, this negative value is not favourable for its bounding with the fibers. Besides its effect being attenuated with the use of cationic starch, an appropriated retention agent should be used to prevent the loss of filler content in the paper. Lourenço *et al.* (2013) indicates CPAM as the indicated retention agent to be used in the application of these particles as paper fillers.

4.2 Coating and Printing Quality

After the characterization process, the next step is to test the modified particles as paper coating pigment. The coating process is described in section 3.2.

Before going through the coating process itself, to better understand which amount of PCC (and posteriorly, of modified particles) is the most suitable to use in this step, coating tests with different ratios starch/PCC were made. The base paper was coated with three different starch/PCC ratios: 1/1, 2/1 and 3/1. The pick-up (difference between the basis weight of the uncoated and coated paper) of the samples was measured, as well as its air permeability and roughness. These results can be found in Appendix F II. The air permeability and the roughness are similar between the three samples. The pick-up increased with the starch/PCC ratio. The ratio 2/1 was found to be the most appropriated to proceed with the coating process, obtaining a pick-up of 5.5.

4.2.1 Coating Properties

After the preliminary tests, sheets of base paper were coated with the modified particles. The solid content of the suspensions used in each sample is about 24 to 26 wt% (a detailed description is presented in Appendix F. II.). For each essay, there were made duplicates and, for the modified particles there were also made replicas.

Before evaluating the printing quality of the coated papers, their pick-up, air permeability and roughness were measured and the results are organized in Table 14. For better understanding, the nomenclature of these samples will be: paper (P) followed by the sample's name, *eg*. P-S2. The base paper (BP), paper coated only with a starch suspension (P-Starch) and paper coated with a suspension of PCC particles (P-PCC) where used as references.

The results of pick-up vs Gurley and pick-up vs roughness are plotted in Figure 16. As it can be seen, the points are too dispersed and there is no linear tendency between the obtained pick-up and the air permeability, as well as the roughness. Although, for P-S2 and P-S6 it is clear that the air permeability increases with the pick-up. In this point, it can be highlighted that for P-S2 with high pick-up, the Gurley test was performed with 50cc due to the long time that was taken to be measured with 100cc. This means that a high pick-up decreases the paper porosity, thus hampering the passage of air. Also, the roughness values for S-P10 and S-P12 show a slightly tendency to increase with the pick-up.
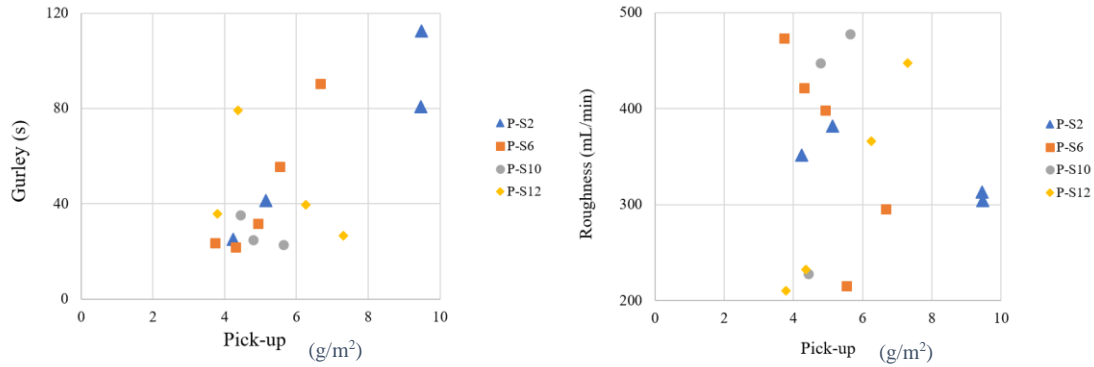
Figure 16. Influence of the pick-up obtained in the paper coating on the air permeability and roughness of the paper

4.2.2 Printing Quality

To evaluate the printing quality, a test mask was printed in each coated paper, and then several parameters were evaluated, such as gamut area and volume, optical density (of cyan, magenta, yellow, and black), print-through, colour-to-colour bleeding among others.

Gamut area and volume values are presented in Table 14. It is possible to see that some of the obtained values are near or higher to those from the base paper. In P-S2 and P-S6 there were obtained values for gamut area higher than 7000. For the same samples the values of gamut volume are also higher. This shows improvements in printing quality when compared with the uncoated paper. However, the replicas for these samples present lower gamut area. This can be explained not only by the difference between the pick-up values, but also by the environmental changes that may have happened when the replicas where made. Thus, to avoid modifications in the rheology of the coating suspension, but also fluctuations during the drying stage, the coating process should be performed under controlled environment.

The gamut area of P-S10 and P-S12 is lower than the one of the base paper. Besides this fact, P-S10 shows better results than P-Starch and P-PCC, which means that these coating particles may also lead to improvement of the printing quality.

As referred, one of the aspects that can influence the printing quality is the pick-up. As plotted in Figure 17 the gamut area of the coated papers P-S2, P-S6, and P-S10 increases with the pick-up. For P-S12 there is no possible conclusion, since the gamut area values are not influenced by the pick-up.

New precipitated calcium carbonate derived for application in papermaking

Table 14. Coating properties and print quality parameters (gamut area and volume, CMYK colours)

Samples	Pick-up (g/m²)	Gurley (s)	Roughness (mL/min)	Gamut Area	Gamut Volume	Cyan	Magenta	Yellow	Black
BP	-	12.0	332.0	6713	148376	0.69	0.87	1.36	1.27
P-Starch	5.1	71.5	380.0	5522	124624	0.57	0.81	1.31	1.28
	2.5	16.7	407.5	5054	110265	0.65	0.71	1.25	1.26
P-PCC	5.9	16.1	264.3	5136	115391	0.65	0.72	1.17	1.25
	5.1	15.7	299.5	5204	116563	0.65	0.73	1.17	1.25
P-S2	9.5	80.8[1]	312.8	7178	166670	0.63	0.91	1.51	1.36
	9.5	113	304.0	7119	167664	0.65	0.84	1.54	1.40
	5.1	41.4	381.5	4687	105635	0.63	0.73	1.13	1.28
	11.4	268[1]	405.2	5764	136443	0.58	0.70	1.37	1.40
	4.2	25.2	351.4	4901	110399	0.62	0.76	1.15	1.27
P-S6	5.5	55.7	215.2	6537	155232	0.66	0.81	1.46	1.43
	6.7	90.5	295.5	7435	177365	0.64	0.97	1.55	1.45
	4.9	31.8	398.0	5999	139055	0.64	0.86	1.28	1.36
	4.3	21.9	421.8	6167	143126	0.63	0.86	1.32	1.35
	3.7	23.6	473.3	5376	122207	0.59	0.78	1.22	1.33
P-S10	4.4	35.2	227.6	5496	126662	0.63	0.70	1.32	1.35
	5.6	22.8	477.5	5612	128277	0.68	0.78	1.20	1.29
	4.8	24.9	447.2	5508	122447	0.68	0.77	1.20	1.26
P-S12	3.8	35.7	209.9	5006	115026	0.58	0.75	1.28	1.33
	4.4	79.2	232.3	5259	120495	0.56	0.74	1.29	1.35
	7.3	26.6	447.2	4998	112084	0.65	0.71	1.25	1.26
	6.3	39.7	366.3	4912	104008	0.64	0.75	1.14	1.16

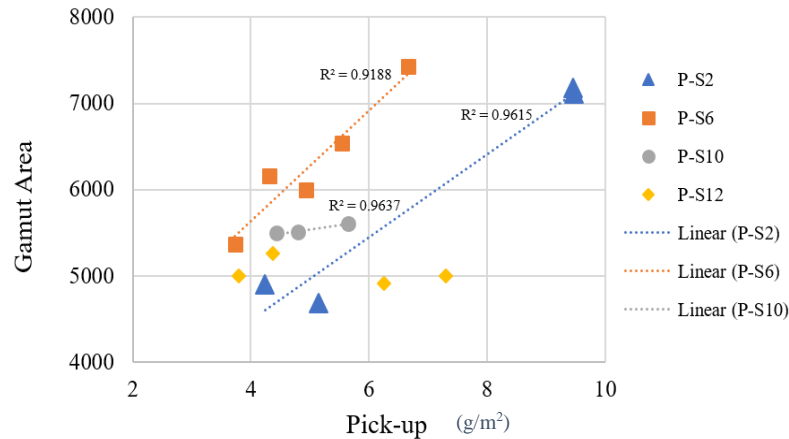[1] The Gurley test was performed with 50cc

Figure 17. Influence of the pick-up on the gamut area

The gamut volume increases with the pick-up for P-S2 and P-S6, as shown in Figure 18. This might be due to the highest optical density of the black colour presented by these paper samples. The remaining samples have lower optical density of the black colour. However, when compared with the base paper, P-S10 shows a slightly improvement.

The optical density of the black and yellow shows also higher values for P-S2 and P-S6, when compared with the base paper. The cyan density is slightly lower than the base paper. However, these two samples show greater results for this property. Relatively to the samples P-S10 and P-S12 the optical density of the colours does not show improvements when compared with the base paper.

The properties of print-through, show-through, black and white (B&W) feathering, and colour-to-colour bleed are compiled in the Table 15.

In the analysis of print and show-though properties it is clear that the presented values are lowered then the ones obtained for PB showing improvements of these parameters when the paper is coated with the modified particles. Compared with the PB, only P-PCC shows higher values of print and show-through, meaning that the ink is more likely to penetrate in the paper when coated with PCC particles than with the modified particles.
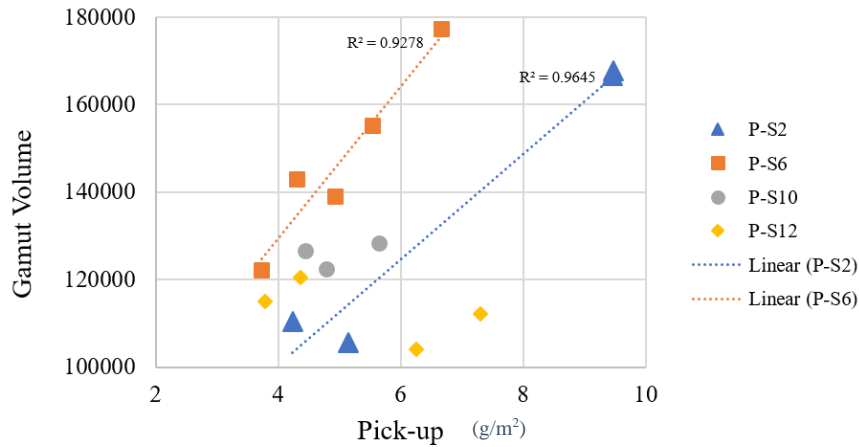
Figure 18. Influence of the pick-up on gamut volume.

The B&W feathering analysis is not that clear, since some papers show improvements while others do not, when compared with PB. However, taking a closer look between samples (Figure 19), the values also vary with the pick-up, showing one more time that the control of the pick-up during the coating process is an important factor. P-S6, P-S10, and P-S12 show that the feathering effect of the line decreases with the increasing of the pick-up. From the analysis of P-S2, there is no correlation to be highlighted.
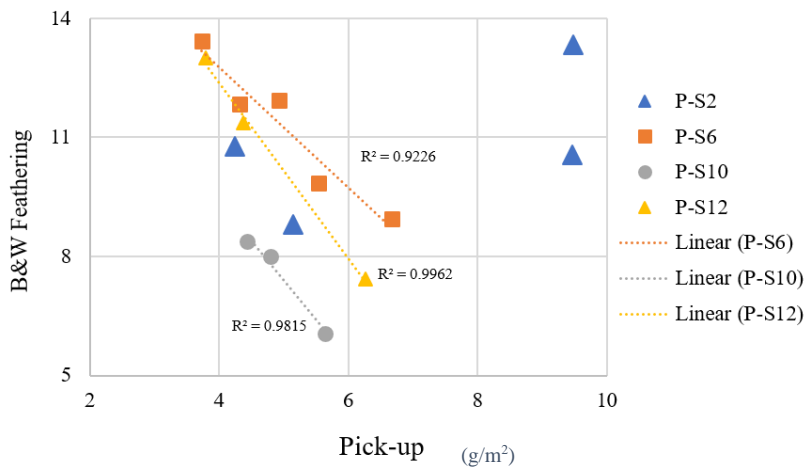
Figure 19. Influence of the pick-up in B&W feathering

Table 15. Print quality properties: print-through, show-through, B&W feathering, and colour-to-colour bleed

Samples	Print-Through	Show-Through	B&W Feathering	Colour-to-Colour Bleed	
				Colour-to-Colour Bleed$_W$	Colour-to-Colour Bleed$_R$
BP	4.3	4.3	10.8	198.1	10.8
P-Starch	3.6	3.6	12.3	109.5	18.3
	4.0	4.0	9.7	90.0	9.0
P-PCC	4.6	4.6	11.7	201.7	8.6
	4.8	4.8	9.8	196.5	9.7
P-S2	2.7	2.7	10.6	103.0	13.3
	2.6	2.6	13.3	62.4	11.7
	3.4	3.4	8.8	102.5	8.8
	2.5	2.5	6.7	84.8	9.5
	3.1	3.1	10.8	106.8	10.3
P-S6	2.8	2.8	9.9	119.7	11.9
	2.8	2.8	8.9	121.2	11.2
	3.7	3.7	11.9	118.5	11.6
	3.1	3.1	11.8	110.7	16.0
	3.2	3.2	13.4	130.8	16.4
P-S10	3.5	3.5	8.4	128.2	9.0
	3.0	3.0	6.1	125.0	10.1
	3.5	3.5	8.0	114.0	8.0
P-S12	3.1	3.1	13.0	122.6	24.0
	2.7	2.7	11.4	132.7	15.7
	2.6	2.6	9.7	90.0	9.0
	3.5	3.5	7.4	62.2	7.4

The colour bleeding is divided in two parameters, the width (W) and raggedness (R) of the line, that are related with the ink absorption into the paper. However, the pick-up does not seem to influence this property. The ink absorption depends on the pigments coating characteristics, which can increase the drying time. The low capacity of absorption increases the probability of the bleeding phenomena to occur. Thus, from the obtained results, it can be pointed out that the modified coating pigments, in their majority, improve this characteristic when a comparison with BP and P-PCC is made.

Another aspect to take into account when the printing quality is being evaluated is the circularity of the black and magenta dots that were printed in the mask. The obtained results are present Table 16. Once again, there is no correlation of the point circularity and the pick-up of the sheets. For this reason, the average values of circularity and colour-to-colour bleed are compared in Table 17. It is noticed that the values improve in the coated papers and those with lower colour-to-colour bleed have also lower circularity. The circularity of magenta dots is improved for P-S2, P-S6 and P-S10, though P-Starch and P-PCC show better definition of these dots.

To sum up the overall obtained results, the printing quality of the coated paper is improved by the modified particles. High values of gamut area and volume were obtained for P-S2 and P-S6. Also, these samples revealed high optical density of CMYK colours. These results are correlated with the pick-up obtained, meaning that this parameter must be adjusted for the improvement of printing quality. The print and show-through capacity were also measured and the papers coated with the modified particles had these parameters decreased.

In regard to line quality, B&W feathering decreases with the increasing of the pick-up for P-S6, P-S10 and P-S12. Also, the colour-bleeding parameter is improved by the coating with the modified particles.

The black and magenta dots have higher definition in P-S2 and P-S12. P-S10 only showed improvements for magenta dots.

There are some aspects that can influence the obtained results, such as the environment conditions, as referred. Also, the coating equipment was adjusted between essays. This can be the cause of the differences found in the replicas of P-S2 and P-S6.

Table 16. Print quality properties: circularity of the black and magenta dots

	Black Dots			Magenta Dots		
	Area (mm²)	Diameter (mm)	Circularity	Area (mm²)	Diameter (mm)	Circularity
BP	0.18	0.48	2.04	0.09	0.31	2.24
P-Starch	0.18	0.47	1.99	0.12	0.38	3.21
	0.18	0.48	1.85	0.14	0.42	1.98
P-PCC	0.19	0.50	1.80	0.11	0.33	1.67
	0.19	0.49	1.69	0.11	0.33	1.71
P-S2	0.18	0.48	1.69	0.16	0.45	1.62
	0.18	0.48	1.67	0.15	0.44	2.09
	0.19	0.49	1.77	0.11	0.33	1.81
	0.18	0.47	1.74	0.14	0.42	2.10
	0.18	0.48	1.60	0.12	0.39	2.72
P-S6	0.18	0.48	1.77	0.13	0.41	1.94
	0.18	0.48	1.83	0.15	0.44	1.54
	0.18	0.49	1.66	0.14	0.42	2.34
	0.19	0.49	1.77	0.17	0.46	2.14
	0.19	0.49	2.02	0.13	0.41	2.93
P-S10	0.18	0.48	1.85	0.13	0.41	2.06
	0.17	0.46	2.24	0.11	0.34	1.30
	0.18	0.48	1.68	0.05	0.16	1.01
P-S12	0.19	0.49	1.80	0.13	0.41	3.36
	0.19	0.49	1.83	0.14	0.42	2.63
	0.18	0.48	1.85	0.14	0.42	1.98
	0.17	0.47	1.62	0.12	0.39	2.48

Table 17. Colour-to-colour Bleed and black dots circularity

Samples	Colour-to-Colour Bleed	Circularity
PB	198.1	2.04
P-Starch	99.73	1.92
P-PCC	199.1	1.75
P-S2	91.91	1.70
P-S6	120.2	1.81
P-S10	122.4	1.92
P-S12	101.9	1.78

4.2.3 Coating characterization

To understand what went wrong with coating replicas, especially P-S2 and P-S6 (with the highest gamut values) the coated paper was analysed by SEM. Figure 20 shows the first attempt of coating paper with the particles S2 and its replica. It is noticed that the particles of the replica have different morphology, meaning that something went wrong with the reaction process, causing the decrease of the gamut area. Figure 21 shows the base paper coated with particles S6, revealing the lamellar shape of the particles. The coated paper matrix for each sample is presented in Figure 22. It is notorious that the particles cover most of the paper matrix, and P-S2 had a denser coverage than P-S6, justifying the high pick-up obtained for P-S2.

However more replicas are needed to prove that these particles, made with citrate buffer, can really improve the printing quality of the papers.
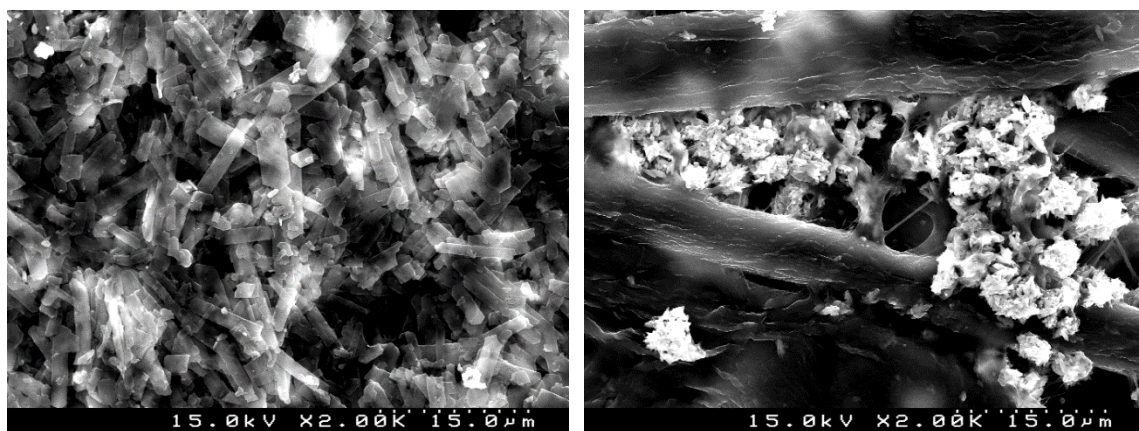
Figure 20. Coated paper with S2 particles (left) and its replica (right). Magnification 2k x.
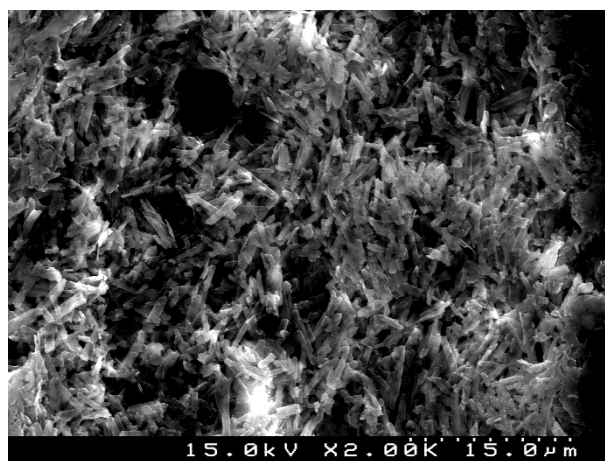
Figure 21. Coated paper with S6 particles. Magnification 2k x.
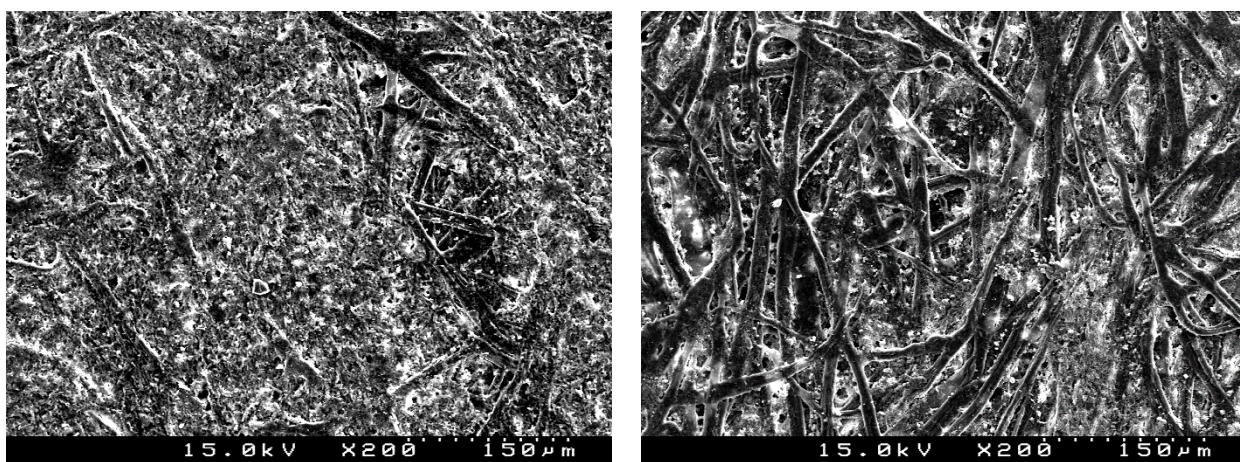
Figure 22.Coated paper matrix. P-S2 (left) and P-S6 (right)

4.3   Paper testing

After testing the modified particles as pigment coating, the next step was to use it as paper filler. The sheets formation was performed in RAIZ as well as its posterior characterization. The evaluation of the loading content in each sheet was evaluated in DEQ.

4.3.1   Handsheets Characterization

Filler Retention

The mineral loading of the produced handsheets was determined following the standard TAPPI 211, and the content and percentage of retention was calculated by the Equations 4.3 and 4.4, respectively.

$$Filler\ content\ (wt\%) = \frac{Ash\ weight\ at\ 525\ °C}{Weight\ of\ paper\ at\ 105\ °C} \times 100 \qquad (4.3)$$

$$\%\ Filler\ retention = \frac{Filler\ content\ (wt\%)}{PCC\ added\ (wt\%)} \qquad (4.4)$$

The retention values are presented in Table 18. For better understanding, the nomenclature of the fillers will be: sheet (S) following the modified particle used as filler, eg. S-S2. The reference will be named as S-PCC for the sheet with PCC filler and a basis weight of 80g/m². As it is noticed, the sheets with the modified particles have lower percentage of retention. For this reason, and to make a better comparison between sheet samples, another sheet reference was produced with PCC filler, though with an average basis weight comparable to those produced with the modified fillers. This sample will be named S-PCC1.

The target filler content in the sheets was 30 wt% and as it can be seen, only the PCC particles reached approximately that value.

The retention is related with the entanglement of the filler with the fibers, and usually CPAM promotes filler retention. The connection between the fibres and PCC is due to their opposite charges: fibres have negative charge and PCC, has positive charge, as seen previously. The attraction between the PCC particles and the fibers is improved with CPAM.

Table 18. Filler content and retention

Sample	Filler content (wt%)	Filler retention (%)
S-PCC	24.8	82.5
S-PCC1	26.3	87.7
S-S2	3.60	12.1
S-S6	4.30	14.2
S-S10	4.90	16.3
S-S12	1.40	4.77

The modified particles present (high) negative surface charge and it is expected that the affinity towards the fiber decreases, leading to low retention values. Actually, this can be seen in Figure 23, where it is plotted a linear correlation between the zeta potential of the modified particles (Table 13) and the filler content values.
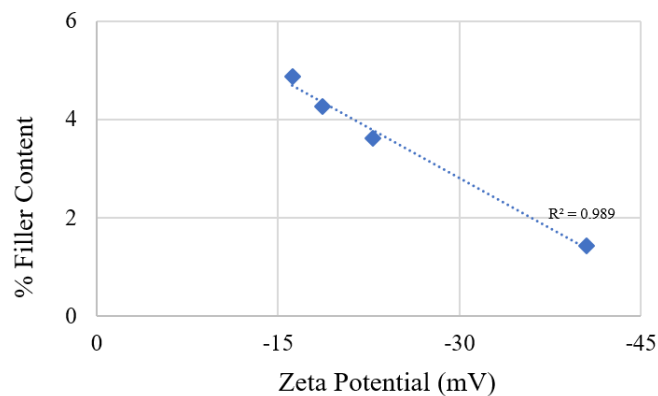
Figure 23. Zeta Potential and Filler content

Although Lourenço *et al.* (2013) had reported that the efficiency of CPAM with highly negative charged particles, the same was not observed in this study. This means that the amount of CPAM may not be sufficient to compensate the particle charge in order to create bonds with the fibers. Also, CPAM may not be the adequate retention agent to use on these modified particles. This aspect requires further studies to evaluate what can be altered in order to increase the mineral loading retention, namely flocculation studies by LDS using only the modified particles and a polyelectrolyte.

Paper properties

After the evaluation of the filler retention, the paper properties were evaluated. In Table 19 the results of each property associated with each kind of filler used, are presented.

As it was expected, the grammage of the sheets with the modified samples decreases with the filler content in the sheets. The bulk and permeability properties follow the same behaviour. In comparison with the references, for the sheets with modified filler, the bulk decreases and the air resistance increases. This is due to the lower mineral content in the sheets, increasing fiber bounding and thus closing the paper matrix.

The roughness of the paper with the modified fillers is also lower than the references, however S-S6 presents a higher value for this property. This is probably due to the large agglomerates present in the particles sample. Comparing the remaining samples, the roughness decreases with the increasing of the filler content, most certainly because the mineral particles fill some of the surface pours. On the other hand, it is too soon to predict if these modified particles contribute to smooth the paper's surface.

The optical properties are related with the interaction of the light with the paper constituents, such as fiber and mineral loading. The fiber refining is a factor to take into account when these properties are evaluated. However, the refining degree is the same in all the sheets in study. Thus, the optical properties are strongly dependent on the filler content. It is noticed (Figure 24 and Table 19) that the sheets with the modified fillers present lower values for opacity and light scattering when compared with the reference S-PCC1. The brightness values present the same tendency, however S-S6 has the same value as S-PCC.
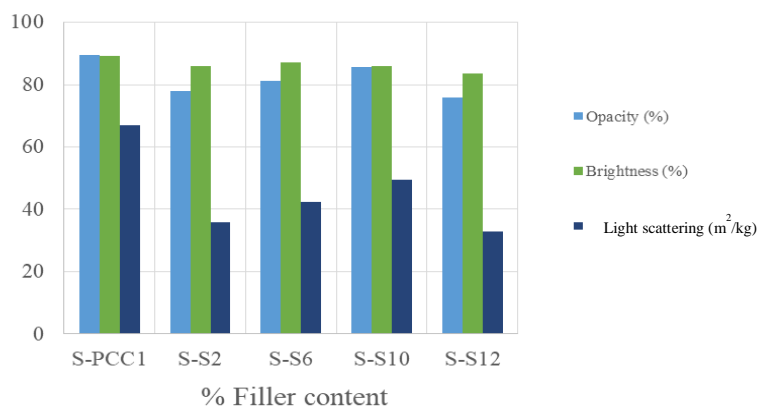
Figure 24. Influence of the filler content in optical properties

Table 19. Paper properties: Structural, optical and mechanical

	Properties	S-PCC	S-PCC1	S-S2	S-S6	S-S10	S-S12
Structural	**Grammage** (g/m²)	80.8	67.1	65.6	66.9	69.1	63.1
	Bulk (cm³/g)	1.7	1.6	1.4	1.4	1.4	1.4
	Permeability (s/mL)	2.3	2.0	5.3	4.5	5.7	4.5
	Roughness (mL/min)	241.6	243.8	167.3	275.7	152.6	183.3
Optical	**Opacity** (%)	91.2	89.5	77.9	81.0	85.6	75.7
	Brightness (%)	87.6	89.3	85.9	87.1	85.8	83.7
	Light Scattering (m²/kg)	66.0	67.0	35.7	42.4	49.6	32.8
Mechanical	**Tensile strength** (kN/m)	23.4	21.2	48.4	38.4	37.4	47.9
	Burst strength (%)	1.4	1.2	3.3	2.3	2.1	2.9
	Tear Resistance (mK)	3.9	1.7	7.5	5.5	5.7	7.6
	Internal resistance (KPa)	184.3	204.8	714.0	399.0	315.0	529.2

The opacity, brightness and light scattering have some tendency to increase with the filler content. This is normal, since the light has more obstacles to be dispersed. Figure 25 shows a linear correlation between opacity and light scattering, which is also in agreement with the trend of light scattering with grammage (Figure 26), reinforcing the influence of the filler content with these properties.
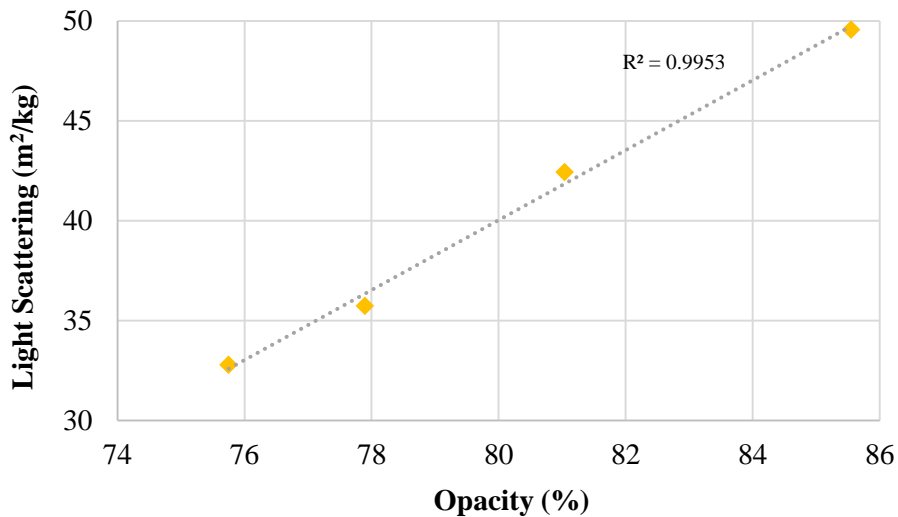
Figure 25. Light scattering vs Opacity
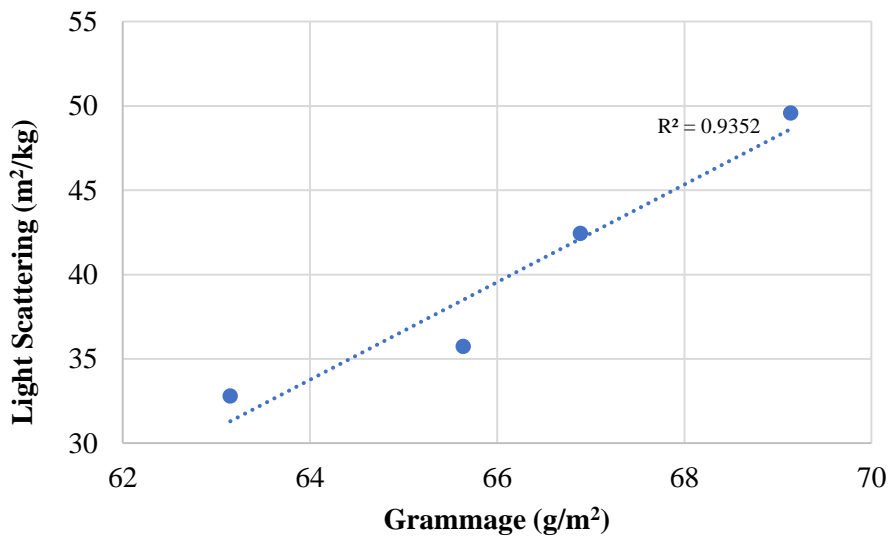
Figure 26. Light Scattering vs Grammage

The mechanical properties increase for the modified particles relatively to the reference PCC-1. This is due to the low filler content of the sheets with the modified filler which increases the fiber-to-fiber bounding. The filler content of PCC-1 is higher, decreasing the bounding between fibers, and thus being less resistance to mechanical tests.

Although, S-S2 has not the lowest filler content but has the highest values for mechanical properties. This can be related to the lamellar morphology that, once again, increases the filler-to-fiber bounding.

The tensile strength and the tear resistance have the same behaviour, when compared between the modified samples. As shown in Figure 27, the tensile and burst strength have a linear correlation, as it was expected.
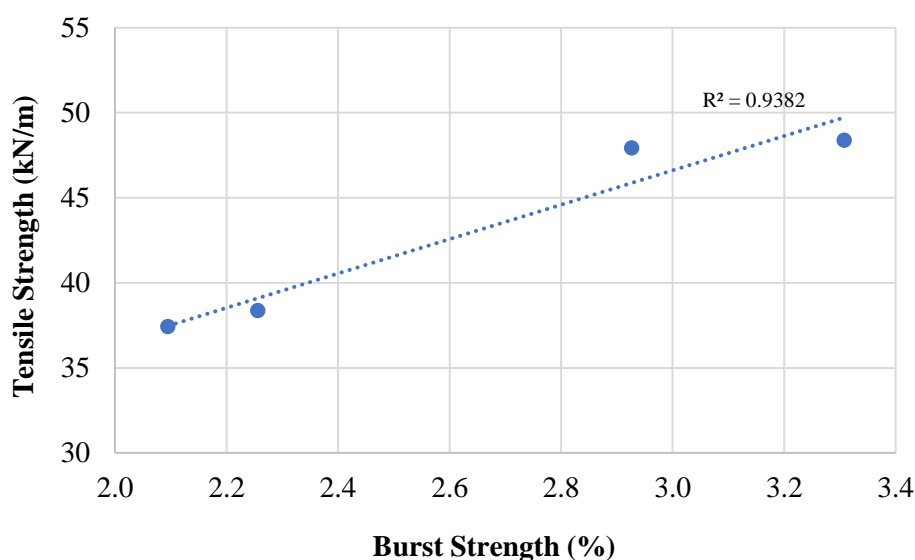
Figure 27. Tensile Strength vs Burst Strength

To sum up, all the properties are dependent on the filler content of the sheets. Compared with the S-PCC1, the modified particles formed a less permeable sheet, and the roughness was decreased. The optical properties are also disturbed with the use of the modified fillers. The mechanical properties increased due to the low filler content. Although S-S2 have the highest values for these properties, maybe due to the lamellar morphology of the particles. In fact, when comparing with S-S12, which has a much lower filler content, the tensile strength is similar to the one of S-S2. Replicas are needed to really make sure which are the paper properties that will improve with the use these modified fillers.

5 Conclusions

A discover made by Carecho (2016) where a lamellar morphology, interesting from a papermaking point of view, was obtained from the mixture between scalenohedral PCC with citrate buffer, leading to the present dissertation. Thus the aim of this work consisted in the study and optimization of the reaction between PCC and citrate buffer to understand how the lamellar morphology was obtained, and its posterior application as paper coating pigment to evaluate printing quality, as well as its application as paper filler.

A preliminary research, where the influence of the citrate buffer pH and CIT/PCC ratio at 50 °C was studied, indicates that the CIT/PCC ratio is a crucial parameter to the formation of the mentioned particles. The CIT/PCC ratio will influence the final suspension pH, revealing that this is also an important aspect to take into account to obtain lamellar particles. Thus, these particles are favourably formed at a CIT/PCC ratio ca. 4 and a final suspension with a pH 5.5. For better control of the CIT/PCC ratio during the experimental essays, it was created a new protocol, in which instead of the preparation of the sodium citrate buffer, two distinct solutions of CIT (1M) and NaOH (1M) were poured into the PCC suspension. The CIT/PCC ratio was decreased for 2, to obtain the same pH, which also resulted in lamellar particles although with higher aspect ratio.

To test more economic solutions to obtain the same structure, the stoichiometric CIT/PCC ratio (1.4) was used with the absence of NaOH. The pH obtained in the final suspension was ca. 5, and lamellar morphology was also obtained. Other aspect was the use of GCC as starting material. The protocol used was the same as the one used in the first experiment, however the resulted particles presented platy-morphology.

Thus, the lamellar morphology can be obtained at an optimum pH of 5.5 and the CIT/PCC ratio can be controlled, depending on the protocol used. Suspensions with low pH also show the formation of lamellar particles, though with lower aspect ratio; suspensions with high pH did lead to present lamellar particles.

The thermal analysis (calcination and TGA up to 900 °C) revealed that the particles in study are composed in its majority with calcium citrate and ca. 30% of $CaCO_3$. Though there are some unidentified compounds that represent about 10% of the samples composition. These compounds can also be related to this radical modification of the scalenohedral PCC.

LDS analyses revealed that the particle size decreased when compared with the starting material, except for the particles obtained by the modification of GCC that showed an increase

of particle size. The particles of modified PCC have a d_{50} of $3.30 - 3.50\,\mu m$. However, particles with higher aspect ratio seemed to form large aggregates.

Relatively to the particle superficial charge, the PCC modified particles presented negative charge, outside of the stability zone. For the GCC modified particles this parameter showed to increase the suspension stability.

After the characterization process, these particles were applied as coating pigments revealing promising results in printing quality. The PCC particles modified with citrate buffer revealed high values of optical density resulting in high values of gamut area in comparison with the base paper used for coating. The pick-up of these papers was about 7-9, which caused high air permeability. Though the same results were not obtained in replicas made posteriorly. These differences can be caused by fluctuation of the environmental conditions, which may alter the coating suspension properties and the drying conditions, changing in this way the coating surface.

The application of the modified particles as paper fillers did not present good results due to their low retention in the paper matrix. The highly negative zeta values can be related with the filler content: the filler content increases with the particles superficial charge. This can reveal that the use of CPAM as a retention agent is not efficient. The paper properties were evaluated with a reference paper with PCC filler with a similar grammage to those obtained with the use of the modified fillers. These properties are strongly dependent of the filler content in the sheets, and thus the mechanical properties increased relatively to the reference. However, it is noticed an improvement of these properties when lamellar particles are used as filler. As expected, the optical properties decreased. The air permeability increased due to the lack of filler, allowing the fibers to form a closer matrix. Thus, there is no conclusions to be taken from these tests.

6 Future Work

In a future work, the next step to be done is the replicas of all the reactions where the lamellar particles were obtained to confirm these results. It is also important to test the influence of the temperature in these reactions.

A more complete particle characterization should be done, namely related with elemental analysis, since as concluded there are some unidentified compounds presented in the analysed samples. Analysis related with the structural mineralogy should be done, such as XDR (*X-Ray Diffraction*) to understand the special arrangement of the crystalline structure. The refractive index and the hydrophobicity of the particles should also be measured.

As the application of these particles as paper filler did not lead to results due to their low retention, it is important to study if the CPAM is the adequate retention agent, or if it is necessary to increase its amount to promote higher retention. Also flocculation studies should be made to better understand the behaviour of these particles during paper formation.

Relatively to the application of these particles as coating pigment, the coater should be fixed to have a correct distance between the paper surface and the rod, resulting in a more accurate pick-up. Also, replicas of the previous coatings should be made.

The use of these particles as coating pigments revealed good results related to printing quality. An economic study in a laboratorial scale should be done to see if a scale up of this process is viable.

7 References

Al-Khaldi, M. *et al.* (2003) 'New Findings on Damage Potential, Geochemical Reaction Mechanisms, and Production Enhancement Applications for Citric Acid', *SPE Journal*, 10(3), pp. 13–14. doi: 10.2118/82218-PA.

Al-Khaldi, M. H. *et al.* (2007) 'Reaction of citric acid with calcite', *Chemical Engineering Science*, 62(21), pp. 5880–5896. doi: 10.1016/j.ces.2007.06.021.

Altay, E., Shahwan, T. and Tanoğlu, M. (2007) 'Morphosynthesis of CaCO3 at different reaction temperatures and the effects of PDDA, CTAB, and EDTA on the particle morphology and polymorph stability', *Powder Technology*, 178(3), pp. 194–202. doi: 10.1016/j.powtec.2007.05.004.

Alyamani, A. and Lemine, O. M. (2012) 'FE-SEM Characterization of Some Nanomaterial', *Scanning Electron Microscopy*, (1), pp. 463–472. doi: 10.5772/34361.

Apelblat, A. (1993) 'Solubilities of organic salts of magnesium, calcium, and iron in water', *The Journal of Chemical Thermodynamics*, pp. 1443–1445. doi: http://dx.doi.org/10.1006/jcht.1993.1145.

Apelblat, A. (2015) *Citric Acid*, *Book*. doi: 10.1017/CBO9781107415324.004.

Au, C. O. and Thron, I. (1995) *Applications of Wet-End Paper Chemistry*. First. Gloucester: Springer-Science+Business Media, B.V.

Bajpai, P. (2015) *Pulp and Paper Chemical.*, *Pulp and Paper Industry*. doi: 10.1016/B978-0-12-803408-8.00003-2.

Biermann, C. J. (1996) *Pulping and*. second. Edited by Elsevier. London: Academic Press.

Bundy, W. M. and Ishley, J. N. (1991) 'Kaolin in paper filling and coating', *Applied Clay Science*, 5(5–6), pp. 397–420. doi: 10.1016/0169-1317(91)90015-2.

Caner, E., Farnood, R. and Yan, N. (2006) 'Effect of the coating formulation on the gloss properties of coated papers', *... Printing and Graphic Arts Conference, Miami* .

Carecho, A. S. (2016) 'Recuperação de cargas minerais de papéis de impressão e escrita por tratamentos alternativos à calcinação', *Master Thesis, University of Coimbra*.

Chatelain, J. C., Silberberg, I. H. and Schechter, R. S. (1976) 'Thermodynamic Limitations in

Organic-Acid/Carbonate Systems', *Society of Petroleum Engineers Journal*, 16(4), pp. 189–195. doi: 10.2118/5647-PA.

Chen, J. and Xiang, L. (2009) 'Controllable synthesis of calcium carbonate polymorphs at different temperatures', *Powder Technology*. Elsevier B.V., 189(1), pp. 64–69. doi: 10.1016/j.powtec.2008.06.004.

Chen, X., Qian, X. and An, X. (2011) 'Using Calcium Carbonate Whiskers As Papermaking', *BioResources*, 6(3), pp. 2435–2447.

Cheng, B. *et al.* (2004) 'Preparation of monodispersed cubic calcium carbonate particles via precipitation reaction', *Materials Letters*, 58(10), pp. 1565–1570. doi: 10.1016/j.matlet.2003.10.027.

Chernyaev, A. and Enberg, E. (2015) 'The use of microcellulose in papermaking', (June), p. 94.

Dedavid, B. A., Gomes, C. I. and Machado, G. (2007) 'MICROSCOPIA ELETRÔNICA DE VARREDURA - Aplicações e preparação de amostras - Materiais Poliméricos, metálicos e semicondutores', *Dados Internacionais de Catalogação na Publicação (CIP)*, p. 60. doi: 10.1017/CBO9781107415324.004.

Ek, M., Gellerstedt, G. and Henriksson, G. (2009) *Pulp and Paper Chemistry and Technology*. Berlin: Deutsche Nationalbibliothek.

El-Sheikh, S. M. *et al.* (2013) 'Effects of cationic surfactant during the precipitation of calcium carbonate nano-particles on their size, morphology, and other characteristics', *Colloids and Surfaces A: Physicochemical and Engineering Aspects*. Elsevier B.V., 422, pp. 44–49. doi: 10.1016/j.colsurfa.2013.01.020.

Gamelas, J. A. F., Lourenco, A. F. and Ferreira, P. J. (2011) 'New modified filler obtained by silica formed by sol-gel method on calcium carbonate', *Journal of Sol-Gel Science and Technology*, 59(1), pp. 25–31. doi: 10.1007/s10971-011-2456-1.

Gane, P. A. C. and Ag, O. 'Mineral Pigments for Paper ':, 3.

Gerardo, B., George, B. and Marten, B. (2004) 'Acid Fracturing With Encapsulated Citric Acid', *Proceedings of SPE International Symposium and Exhibition on Formation Damage Control*, pp. 0–3. doi: 10.2523/86484-MS.

Geyssant, J. (2003) *Calcium carbonate: from the Cretaceous period into the 21. century*,

Reviews in Mineralogy and Geochemistry. Edited by F. W. Tewthor. doi: 10.2113/0540057.

Holik, H. (2013) *Handbook of Paper and Board*. Germany: Wiley-VCH.

Hu, Z., Shao, M., Li, H., *et al.* (2009) 'Synthesis of Needle-Like Aragonite Crystals in the Presence of Magnesium Chloride and Their Application in Papermaking', *Advanced Composite Materials*, 18(4), pp. 315–326. doi: 10.1163/156855109X434720.

Hu, Z., Shao, M., Cai, Q., *et al.* (2009) 'Synthesis of needle-like aragonite from limestone in the presence of magnesium chloride', *Journal of Materials Processing Technology*, 209(3), pp. 1607–1611. doi: 10.1016/j.jmatprotec.2008.04.008.

Hubbe, M. A. and Gill, R. A. (2016) 'Fillers for Papermaking : A Review of their Properties, Usage Practices, and their Mechanistic Role', *BioResources*, 11, pp. 2886–2963.

Imerys (2017) *Business paper*. Available at:www.imerys.com. (Accessed: 12 April 2017).

Inc., M. T. (2017) *Precipitated Calcium Carbonate.* Available at: www.mineralstech.com (Accessed: 12 April 2017).

Jimoh, O. A., Okoye, P. U., *et al.* (2017) 'Continuous synthesis of precipitated calcium carbonate using a tubular reactor with the aid of aloe vera (Aloe barbadensis Miller) extract as a green morphological modifier', *Journal of Cleaner Production*. Elsevier Ltd, 150(March), pp. 104–111. doi: 10.1016/j.jclepro.2017.02.200.

Jimoh, O. A., Ariffin, K. S., *et al.* (2017) 'Synthesis of precipitated calcium carbonate: a review', *Carbonates and Evaporites*. Springer Berlin Heidelberg, pp. 1–16. doi: 10.1007/s13146-017-0341-x.

Karar, A., Naamoune, F. and Kahoul, A. (2016) 'Chemical and electrochemical study of the inhibition of calcium carbonate precipitation using citric acid and sodium citrate', *Desalination and Water Treatment*. Taylor & Francis, 57(35), pp. 16300–16309. doi: 10.1080/19443994.2015.1077743.

Laufamann, M. *et al.* (2000) 'GCC vs. PCC as the Primary Filler for Coated and Uncoated Woodfree Paper, 1998 Papermakers Conference Proceedings', *Tappi*.

Lin, C. *et al.* (2016) 'Effects of Single and Blended Coating Pigments on the Inkjet Image Quality of Dye Sublimation Transfer Printed Paper : SiO 2 , CaCO 3 , Talc , and Sericite', 2016.

Linseis (2012a) 'Differential Scanning Calorimetry (DSC) / Differential Scanning Calorimeter'. Available at: https://www.linseis.com.

Linseis (2012b) *Thermogravimetry (TGA)*. Available at: https://www.linseis.com.

Lourenço, A. F. *et al.* (2013) 'Evaluation of silica-coated PCC as new modified filler for papermaking', *Industrial and Engineering Chemistry Research*, 52(14), pp. 5095–5099. doi: 10.1021/ie3035477.

Mansour, S. A. A. (1994) 'Thermal decomposition of calcium citrate tetrahydrate', *Thermochimica Acta*, 233(2), pp. 243–256. doi: 10.1016/0040-6031(94)85118-2.

Martin, T. (2005) 'Navigating the Digital Ink Jungle', *S G I A J o u r n a l*, pp. 5–11.

Meldrum, F. C. and Hyde, S. T. (2001) 'Morphological influence of magnesium and organic additives on the precipitation of calcite', *Journal of Crystal Growth*, 231(4), pp. 544–558. doi: 10.1016/S0022-0248(01)01519-6.

Mesic, B. B. and Johnston, J. H. (2013) 'Inkjet Printability of Newsprint : Effects of Starch-based Coatings', (6).

Morsy, F. A. *et al.* (2015) 'Application of nanostructured titanium dioxide pigments in paper coating: a comparison between prepared and commercially available ones', *Journal of Coatings Technology Research*. Springer US, 13(2), pp. 307–316. doi: 10.1007/s11998-015-9735-7.

Moutinho, I. M. T., Ferreira, P. J. T. and Figueiredo, M. L. (2007) 'Impact of surface sizing on inkjet printing quality', *Industrial and Engineering Chemistry Research*, 46(19), pp. 6183–6188. doi: 10.1021/ie070356k.

Nutbeem, C. and Nutbeem, C. (2013) 'Recent Trends In Coating Pigment Use And Formulation Practice In Asia And Western Markets'.

Omya (2015) *Paper & Board*. Available at: www.omya.com (Accessed: 12 April 2017).

Park, W. K. *et al.* (2008) 'Effects of magnesium chloride and organic additives on the synthesis of aragonite precipitated calcium carbonate', *Journal of Crystal Growth*, 310(10), pp. 2593–2601. doi: 10.1016/j.jcrysgro.2008.01.023.

Radfarnia, H. R. and Iliuta, M. C. (2013) 'Limestone acidification using citric acid coupled with two-step calcination for improving the CO2 sorbent activity', *Industrial and Engineering Chemistry Research*, 52(21), pp. 7002–7013. doi: 10.1021/ie400277q.

Reddy, M. M. and Hoch, A. R. (2001) 'Calcite Crystal Growth Rate Inhibition by Polycarboxylic Acids', *Journal of Colloid and Interface Science*, 235(2), pp. 365–370. doi: 10.1006/jcis.2000.7378.

Sequeira, P. C. (2014) 'Modificação de carbonato de cálcio natural com sílica para aplicações em papel', *Master Thesis, University of Coimbra*.

Singh, M. *et al.* (2010) 'Inkjet printing-process and its applications', *Advanced Materials*, 22(6), pp. 673–685. doi: 10.1002/adma.200901141.

Velho, J. (2003) *Mineral Fillers For Paper Why, What, How*. Tomar: Tecnicelpa Technical books.

Wada, N., Kanamura, K. and Umegaki, T. (2001) 'Effects of Carboxylic Acids on the Crystallization of Calcium Carbonate.', *Journal of colloid and interface science*, 233(1), pp. 65–72. doi: 10.1006/jcis.2000.7215.

Wang, S. *et al.* (2009) 'The effect of base paper and coating method on the surface roughness of pigment coatings', *Journal of Dispersion Science and Technology*, 30(6), pp. 37–41. doi: 10.1080/01932690802646447.

Westin, K. J. and Rasmuson, A. C. (2003) 'Precipitation of calcium carbonate in the presence of citrate and EDTA', *Desalination*, 159(2), pp. 107–118. doi: 10.1016/S0011-9164(03)90063-4.

Xiang, L. *et al.* (2004) 'Formation of CaCO3 nanoparticles in the presence of terpineol', *Materials Letters*, 58(6), pp. 959–965. doi: 10.1016/j.matlet.2003.07.034.

Yu, J. *et al.* (2004) 'Facile preparation of calcium carbonate particles with unusual morphologies by precipitation reaction', *Journal of Crystal Growth*, 261(4), pp. 566–570. doi: 10.1016/j.jcrysgro.2003.09.035.

Zhou, D. *et al.* (1998) 'Synthesis and Characterization of Calcium Carbonate Whiskers', 1(3), pp. 133–135.

Appendices

Appendix A

 PCC Modification Reaction

I. Procedure used by *Carecho* (2016) to modify the PCC particles – Reference procedure, S0.

The procedure used in the previous work followed the presented steps:

1) Add 2 g of industrial PCC in a 400mL beaker, and the add 50 mL of ultrapure water;

2) To homogenize the suspension, it undergoes vigorous magnetic stirring. The suspension is heated gradually up to 50 ℃.

3) Add the citrate buffer solution (prepared as described above) until it reaches the pH 5.5, measured at 50 ℃.

4) Place the mixture in an oil bath at 50 ℃. With the help of the mechanic stirrer, *Heidolph RZR-1*, and a round point glass propeller, it is stirred at 165 rpm for 48h. After, pour the mixture into falcon tubes to undergo centrifugation in the *Hettich Universal 32* equipment. The centrifugation must be done for 20 minutes and at 4500 rpm. This process should be repeated three times with two intermediated washes with distillate water.

5) The obtained solid residue is after dried in the oven (*Scientific series 9000*) at 40 ℃ until it is completely dry.

II.   Citrate buffer 1M and pH 4.5

To prepare 100mL of citrate buffer the following steps must be done:

1) Using a beaker, weight 21g of citric acid;

2) Add 75mL of ultrapure water and stir magnetically until it dissolves completely;

3) Adjust the mixture pH to 4.3 with pellets of NaOH (about 7,5 g needed);

4) Pour the mixture into a volumetric flask (100 mL), fill up with water and stir;

5) Measure again the pH of the solution. If pH 4.5 is not reached yet, add some NaOH until the pH is obtained.

III.   PCC particles modification (optimized process)

1) Add 2 g of industrial PCC in a 400mL beaker, and the add 50 mL of ultrapure water;

2) To homogenize the suspension, it undergoes vigorous magnetic stirring. The suspension is heated gradually up to 50 ºC;

3) Add the citrate buffer solution (prepared as described above) until it reaches the pH 5.5, measured at 50 ºC.

4) When reaction conditions are reached, the mixture remains under stirring for 1h, to make sure that all the of the compounds react;

5) After this time, the mixture is poured into falcon tubes to proceed the centrifugation step in the *Hettich Universal 32* equipment. The centrifugation must be done for 20 minutes and at 4500 rpm. This process should be repeated three times with two intermediated washes with distillate water.

6) The obtained solid residue is after dried in the oven (*Scientific series 9000*) at 40 ºC until it is completely dry.

This procedure was used to produce the particles S2, S3, S8, S11, and S12. In these reactions, the buffer pH is changed. This change is made when the buffer is prepared, by adding more NaOH to increase the buffer's pH.

The particles of S1 were produced with the same protocol, although as it was an attempt to reproduce the reference protocol, the buffer preparation was not yet fully understood. So, in this case, to form the citrate buffer, instead of using pellets of NaOH, it was used a NaOH solution of 0.1M.

IV.   Procedure using a CIT 1M

This protocol requires the preparation of CIT 1M before starting to follow the steps described below.

1) Add 2 g of industrial PCC in a 400mL beaker, and the add 50 mL of ultrapure water;
2) To homogenize the suspension, it undergoes vigorous magnetic stirring. The suspension is heated gradually up to 50 ℃;
3) Add the CIT solution drop-to-drop until with until the desired ratio/pH is reached.
4) When reaction conditions are reached, the mixture remains under stirring for 1h, to make sure that all the of the compounds react;
5) After this time, the mixture is poured into falcon tubes to proceed the centrifugation step in the *Hettich Universal 32* equipment. The centrifugation must be done for 20 minutes and at 4500 rpm. This process should be repeated three times with two intermediated washes with distillate water.
6) The obtained solid residue is after dried in the oven (*Scientific series 9000*) at 40 ℃ until it is completely dry.

This protocol was used to obtain S4, S9, S10 and S13. The ratios and the pH of the final solutions altered between the samples. S10 and S13 have the same protocol except that GCC was used as starting material of S13.

V.   Procedure using a CIT 1M solution and a NaOH 1M solution

This protocol requires the preparation of CIT 1M and NaOH 1M before starting to follow the steps described below.

1) Add 2 g of industrial PCC in a 400mL beaker, and the add 50 mL of ultrapure water;
2) To homogenize the suspension, it undergoes vigorous magnetic stirring. The suspension is heated gradually up to 50 ℃;
3) As the pH of calcium carbonate is close to 9.5, start carefully with the addition of CIT solution drop-to-drop and near the desired pH of 5.5, start controlling it with the NaOH solution until the CIT/PCC ratio is reached.

4) When reaction conditions are reached, the mixture remains under stirring for 1h, to make sure that all the of the compounds react;

5) After this time, the mixture is poured into falcon tubes to proceed the centrifugation step in the *Hettich Universal 32* equipment. The centrifugation must be done for 20 minutes and at 4500 rpm. This process should be repeated three times with two intermediated washes with distillate water.

6) The obtained solid residue is after dried in the oven (*Scientific series 9000*) at 40 ºC until it is completely dry.

These method is used in S5, S6, S7 reaction. The principle of all of these reactions is the same. However, the CIT/PCC ratio can be altered, as well as the pH of the final suspension.

Appendix B

Coating and Printing Quality

I. Native Starch suspension

1) Weight a 100mL beaker with the magnetic bar and tare;

2) In the tared beaker, weight 10g of cationic starch;

3) Pour 37mL of ultrapure water previously heated to 60 ℃;

4) Heat the mixture (water + starch) with vigorous stirring up to 65 ℃ and add more 20 mL of the preheated water to avoid gel formation and facilitate the stirring;

5) Gradually extend heating to 70 ℃ and add 3.3 µm of enzyme (α-amilase) under strong agitation. Once again extend the heating for 5 minutes until the temperature reach 80 ℃;

6) To end the enzymatic conversion, add 1.7 mL of zinc sulfate solution, keeping the mixture under stirring. Heat the suspension up to 90-92 ℃, keeping the stirring at this temperature for 15 minutes (starch's cooking). Ending this time, cool the suspension to 50 ℃ (always under vigorous stirring);

7) The consistency of the suspension is adjusted with warm water (60 ℃), typically to 12 wt%.

Appendix C

Additives and Fiber Preparation

I. PCC suspension

The PCC / modified particles suspension is prepared as following:

1) Weight the amount of particles needed to the sheets production and dilute with water until making a suspension of 1wt%.

2) The suspension undergoes magnetic stirring for 20 min;

3) After this time, take the suspension to ultrasounds for 15 min and then more 20 min of magnetic stirring;

4) Keep the suspension always in agitation.

II. Starch and ASA suspension

1) Weight a 1000mL with a magnetic bar (w_{beaker}) and weight 20g of cationic starch;

2) Add 800mL of demineralized water pre-heated at 60 ºC, to avoid the gel formation and facilitate the agitation;

3) Heat the suspension up to 78 ºC, add 10 μL of α-amylase enzyme and thus starting the hydrolysis. Extend the heating for 5 minutes to 80 ºC;

4) Add 3.3 mL of zinc sulfate to end the enzymatic conversion. Keep the mixture always in stirring;

5) Extend the heating up to 90-92 ºC for 15 minutes (starch's cooking)

6) Cool down to 80 ºC and add 2g of ASA;

7) Keep the suspension temperature between 60 ºC – 70 ºC.

The beaker must be covered to reduce evaporation of water, thus altering the starch concentration.

Before the first use, the beaker must be weighted (w_{total}) to know the exact concentration of starch presented in the suspension (Equation A.1). With the paper formation the starch concentration changes, therefore by the Equation A.2 the exact amount to take out of the suspension is determined, before the paper formation.

$$Concentration \left(\frac{g_{starch}}{g_{suspension}}\right) = \frac{20\ g}{w_{total} - w_{beaker}} \qquad (A.1)$$

$$Amount\ of\ suspension\ to\ be\ added\ = \frac{0.016 \times (w_{total} - w_{beaker})}{(20 - (adding\ number\ \times 0.016)} \qquad (A.2)$$

III.   CPAM

1) Weight 0.1g of Percol ®
2) Add 100 mL of warm water (40 ºC) under stirring until the solid content is completely dissolved. Add the remaining water to make 400g of solution.

To add 0.00032 g it must be taken out 13 μm.

IV.   Fiber consistency determination

1) Disintegrate 30g of dried pulp in 1L of water at 1200 rpm;
2) Prepare a suspension of 8L of disintegrated pulp;
3) Homogenize the pulp suspension and weight in a 500mL beaker (500g of suspension) – register the weight ($w_{suspension}$);
4) Produce a sheet with the beaker suspension: fill the former with water and before it reaches the sensor, pour the fiber suspension. Wash the beaker and pour the washing water into the former;
5) After the stirring, decantation and draining processes, raise the former up and place 3 blotters above the pulp sheet, and a metallic disc;
6) Apply pressure;
7) Remove the metallic disc and the 2 superior blotters. Dry the blotter + sheet set in a dryer;
8) After the sheet is dried, put it into a closed cup and weight it promptly – Register (w_{dried});
9) Repeat all the steps for 2 more pulp sheets;

10) Calculate an average of the 3 weights and determine the consistency by the Equation A.3, to know which amount of suspension is needed to make a sheet with 1.102 g of fiber, Equation A.4.

$$\% \, Fiber \, suspension \, consistency = \frac{w_{dried}}{w_{suspension}} \times 100 \qquad (A.3)$$

$$Amount \, to \, weight \, (g) = \frac{1.102 \times w_{suspension}^{average}}{w_{dried}^{average}} \qquad (A.4)$$

Appendix D

Sheets Formation

The formed sheet is obtained as the following steps:
1) Fill the former with ¾ of water;
2) Place the determined amount of fiber under stirring;
3) Add the needed mineral loading and start the clock counting;
4) At 2 minutes, add amount of the mixture starch + ASA calculated by the Equation A.2 (Appendix A) ;
5) Add the CPAM at minute 4 and 30 seconds;
6) At minute 4 and 35 seconds, remove the magnetic bar and pour the mixture into the former. Wash the beaker and pour the washing water also into the former;
7) Open the former after the stirring, decantation and draining processes. Place two blotters (on new and one used) and a metallic disc above the sheet. Apply pressure;
8) Take the metallic disc and the superior blotter off, and place the sheet + blotter in the pressing machine.

I. Pressing and sheets conditioning

1) Place 2 bottlers in the machine's base. Place the produced sheets alternately with the blotters;
2) End the pile with 2 blotters;
3) Place the machine superior board above the pile and squeeze "in cross";
4) The pile is pressed for 5 minutes. In the end, remove the pile;
5) Place 2 bottlers in the machine's base. Remove the blotters and place a new blotter above each sheet;
6) Press the new pile of sheets for 2 minute. At the end remove the pile.
7) Place the metallic discs and the corresponding sheets into the drying rings in the conditioning room. Place the pile of rings near the fan;
8) After the sheets' drying (2h minimum), separate the discs from the sheets and place the sheets into the adequate place in the conditioning room to proceed with the characterization stage.

Appendix E

Particles Characterization

I. Optical Microscopy Images

After the optical microscopy analysis, some pictures were taken from each reaction and are presented below.
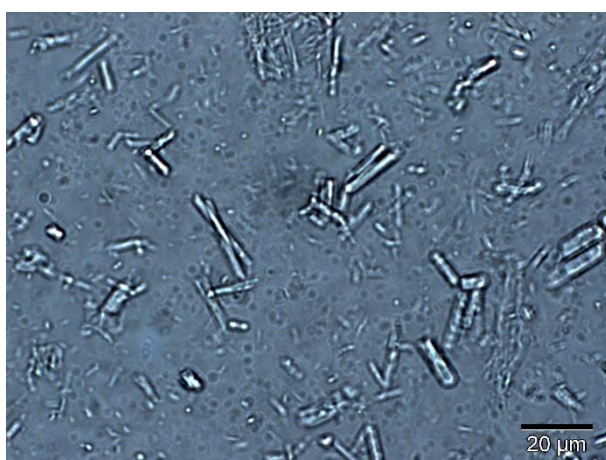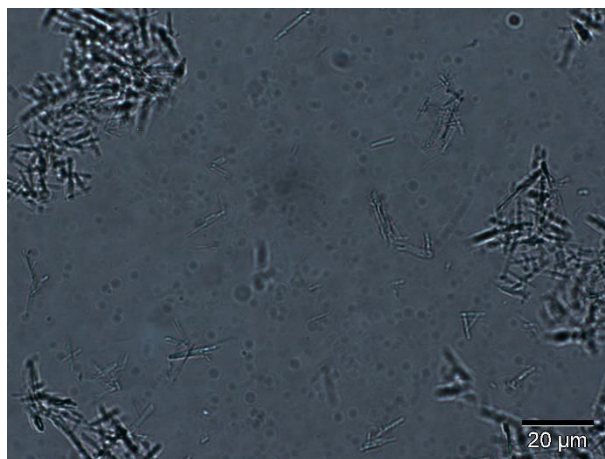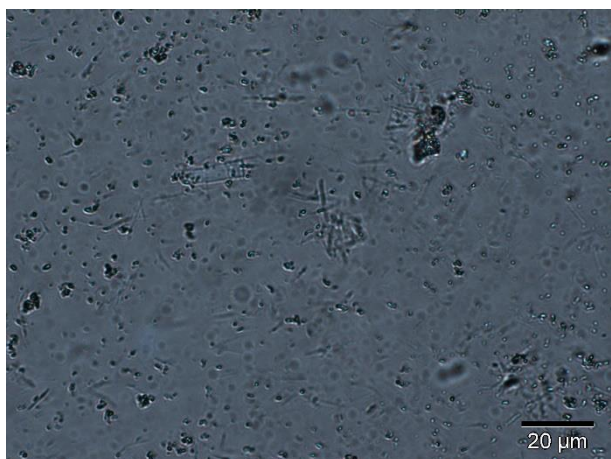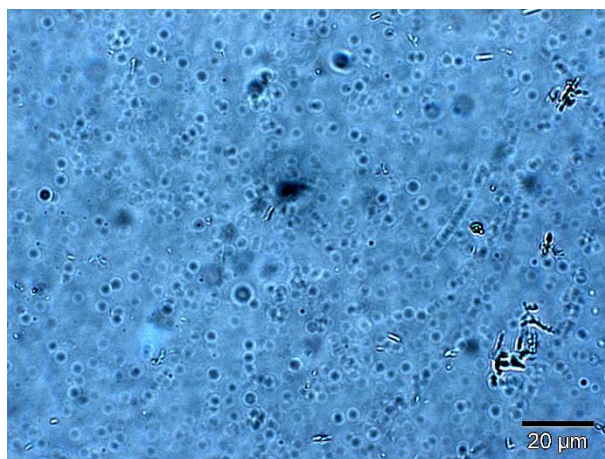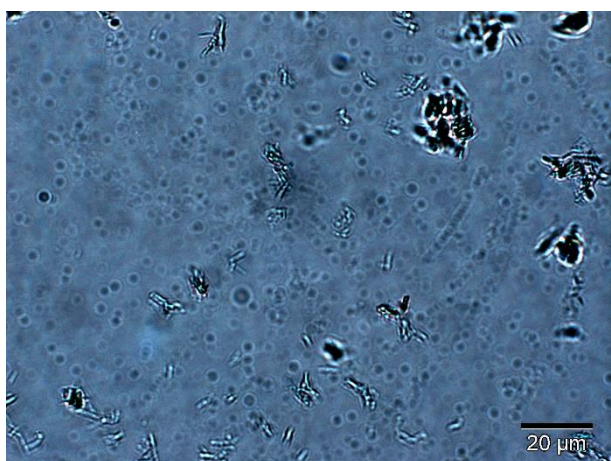

Figure E1. S1 particles. Magnification: 50x.
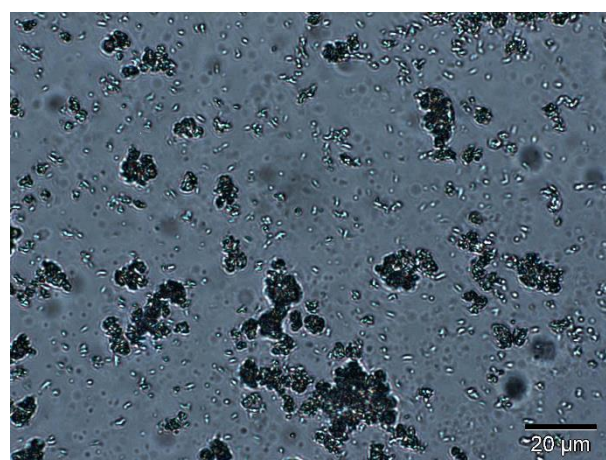
Figure E2. S3 particles. Magnification 50x
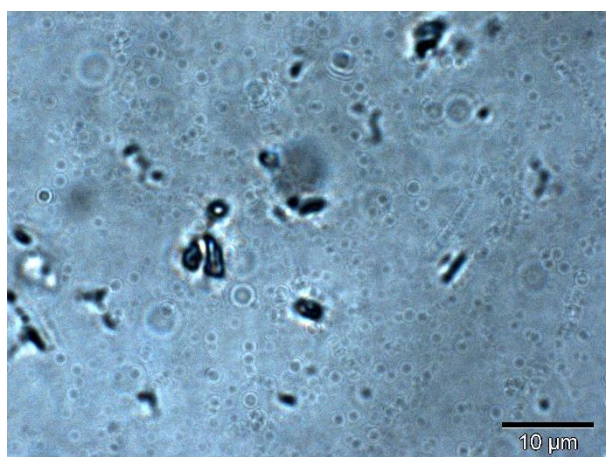
Figure E3. S4 Particles. Magnification 50x
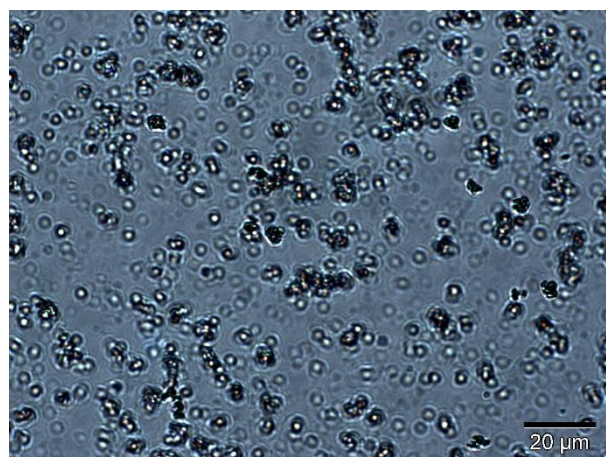
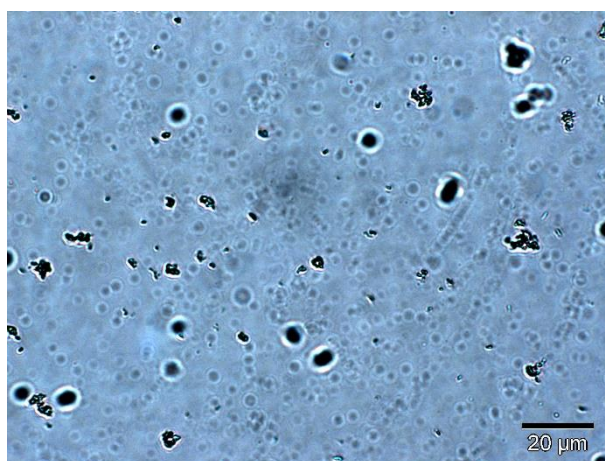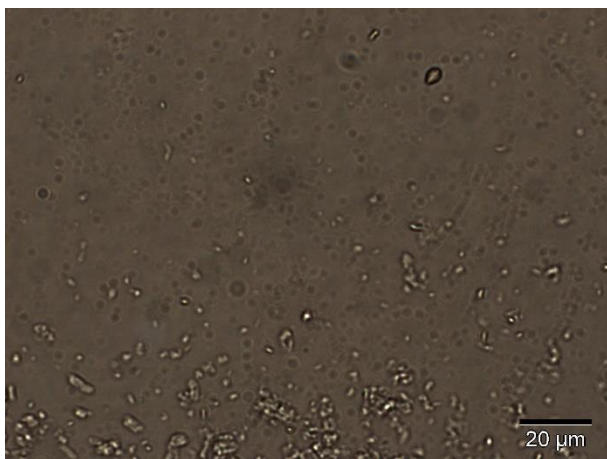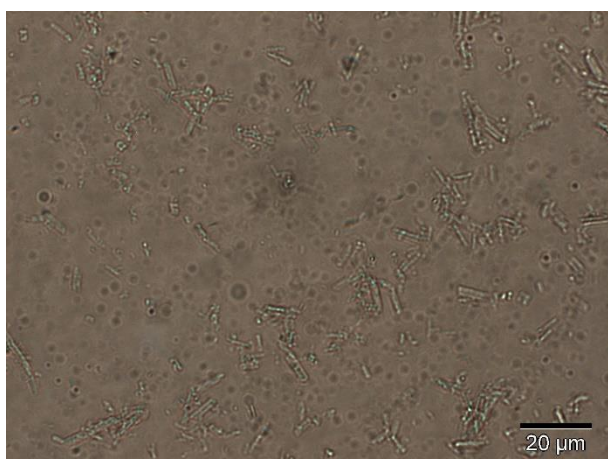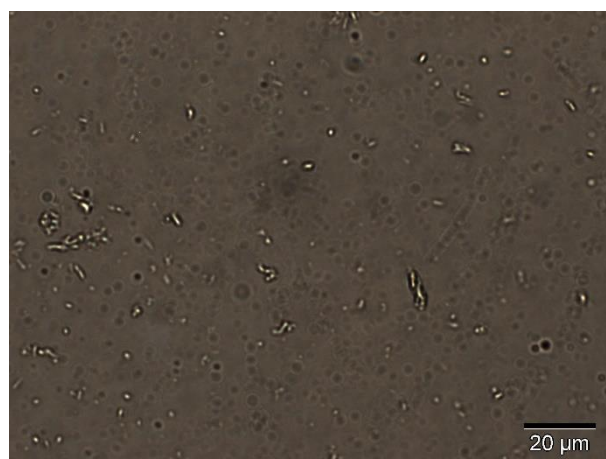Figure E4. S5 Particles. MAginifcation 50x
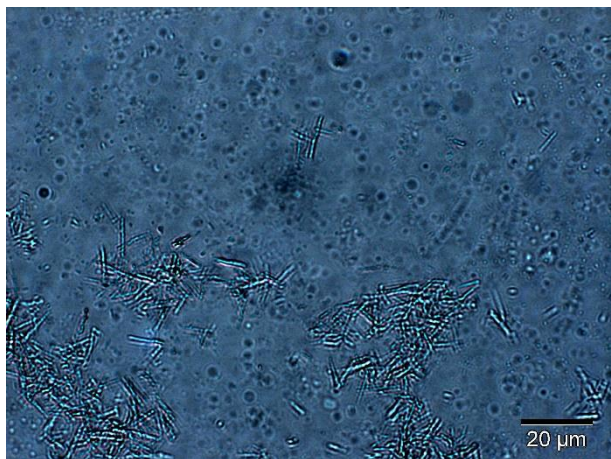
Figure E5. S6 particles. Magnification 50x

Figure E6. S7 Particles. Magnification 50x

Figure E7. S8 Particles. Magnification 50x.

Figure E8. S9 Particles. Magnification 50x.

Figure E9. S10 Particles. Magnification 50x.
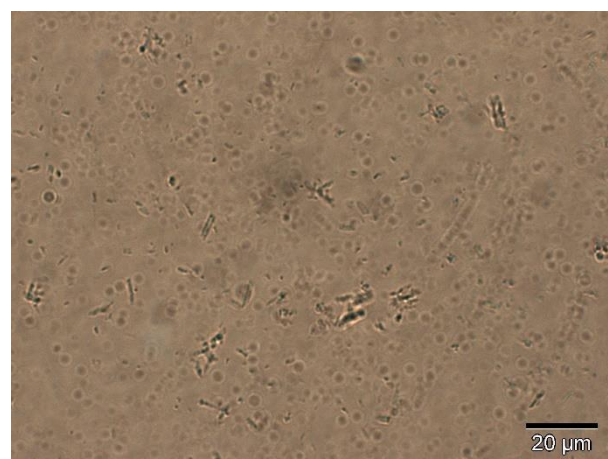

Figure E10. S11 Particles. Magnification 50x.

E.2

Figure E11. S12 Particles. Magnification 50x.

II.   Coating Particles

Figure E12. S6 coating particles. Magnification 50x.

Figure E13. S10 coating particles. Magnification 50x.

Figure E14. S12 Coating Particles. Magnification 50x.

Figure E15. S2 coating particles. Magnification 50x.

Reaction Process yield

Table E1. Process reaction yield

	Sample	2	6	10	12
Reactants Amount (g)	**CIT**	8.40	4.00	4.20	12.6
	NaOH	7.20	0.41	-	4.67
	PCC	2.00	2.00	3.00	2.00
	Total	17.6	6.41	7.20	19.27
	CIT/PCC Ratio	4.20	2.00	1.40	6.30
	Product amount	3.10	5.40	4.00	3.00
	Yield (%)	18.0	84.0	56.0	16.0

III. SEM Images
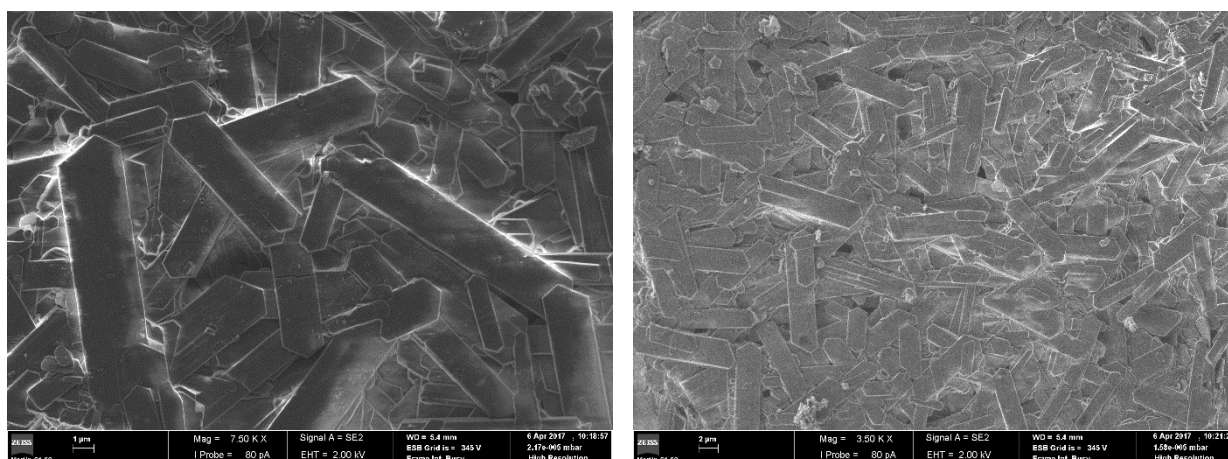
Figure E16. S2 SEM images. Magnification 7.50k (left) and 3.50k (right)
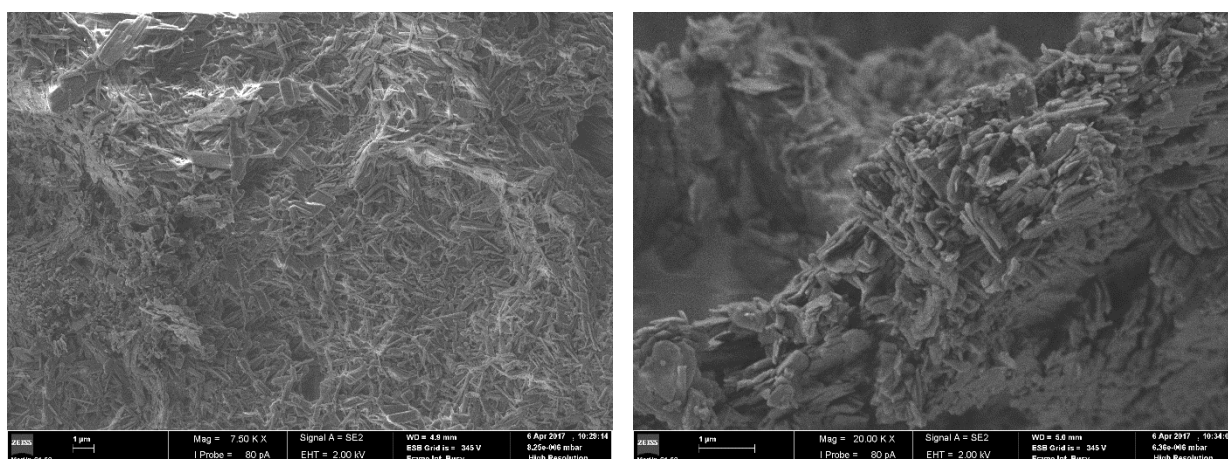
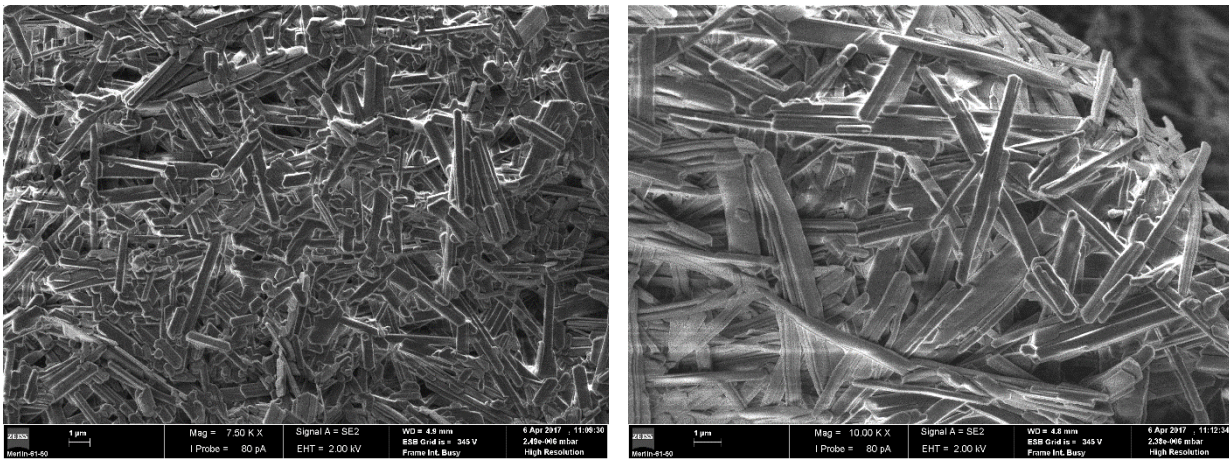Figure E17. S4 SEM images. Magnification 7.50k (left) and 20.0k (right)

Figure E18. S6 SEM images. Magnification 7.50kx (left) and 10kx (right)
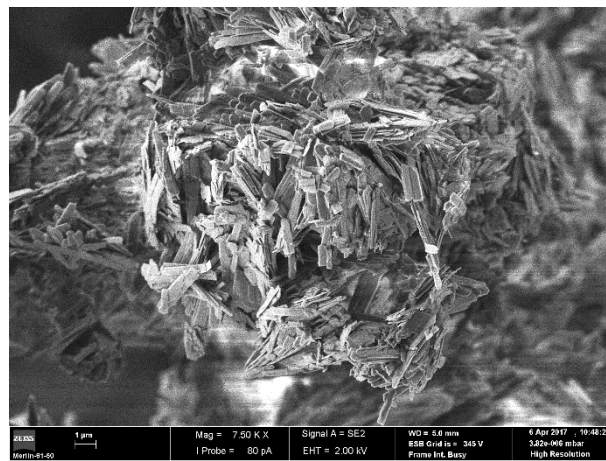

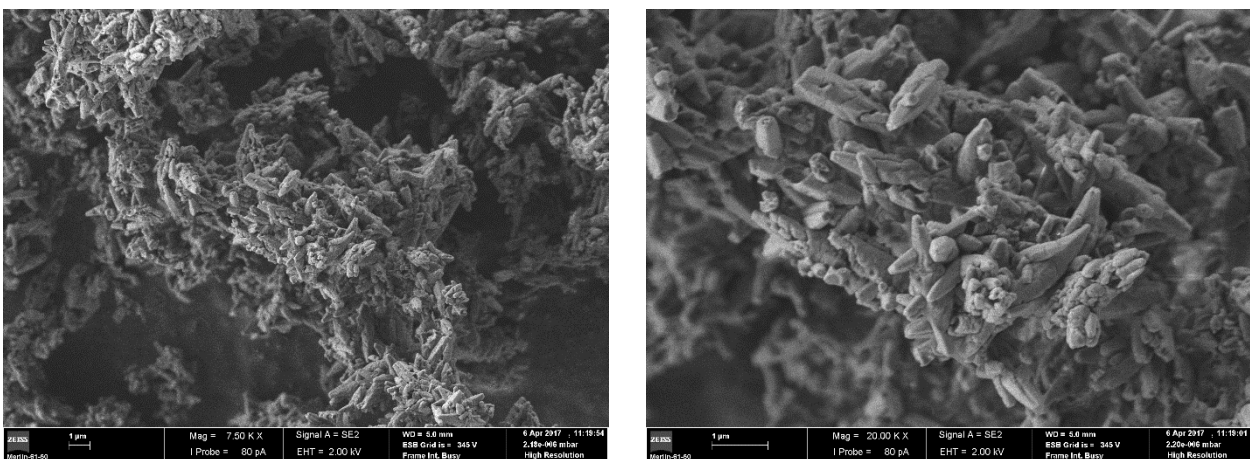Figure E19. S10 SEM image. Magnification 7.50k x.

Figure E20. S11 SEM images. Magnification 7.50k x (left) and 20.0k x (right)
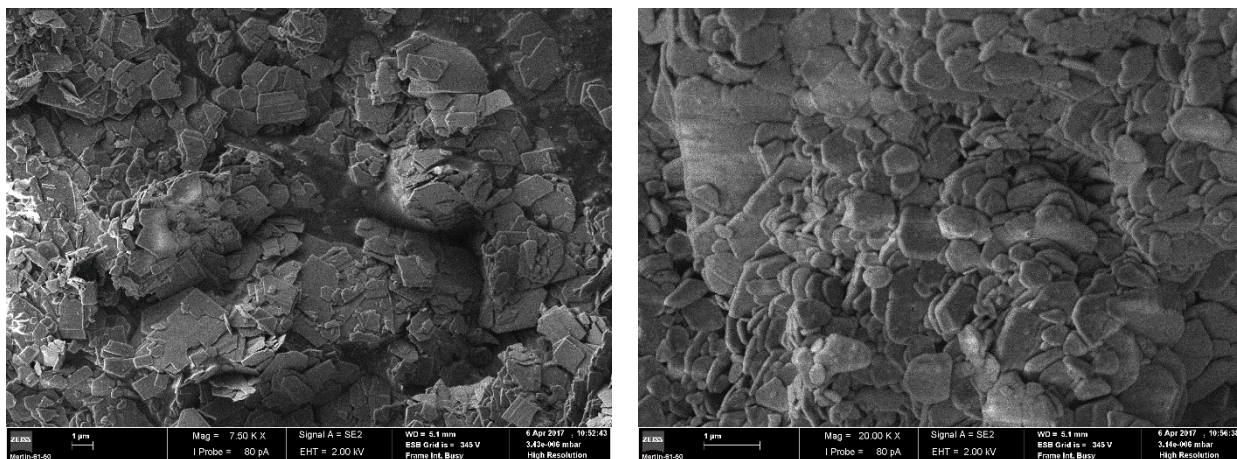
Figure E21. S12 SEM images. Magnification 7.50k x (left) and 20.0k x (right)
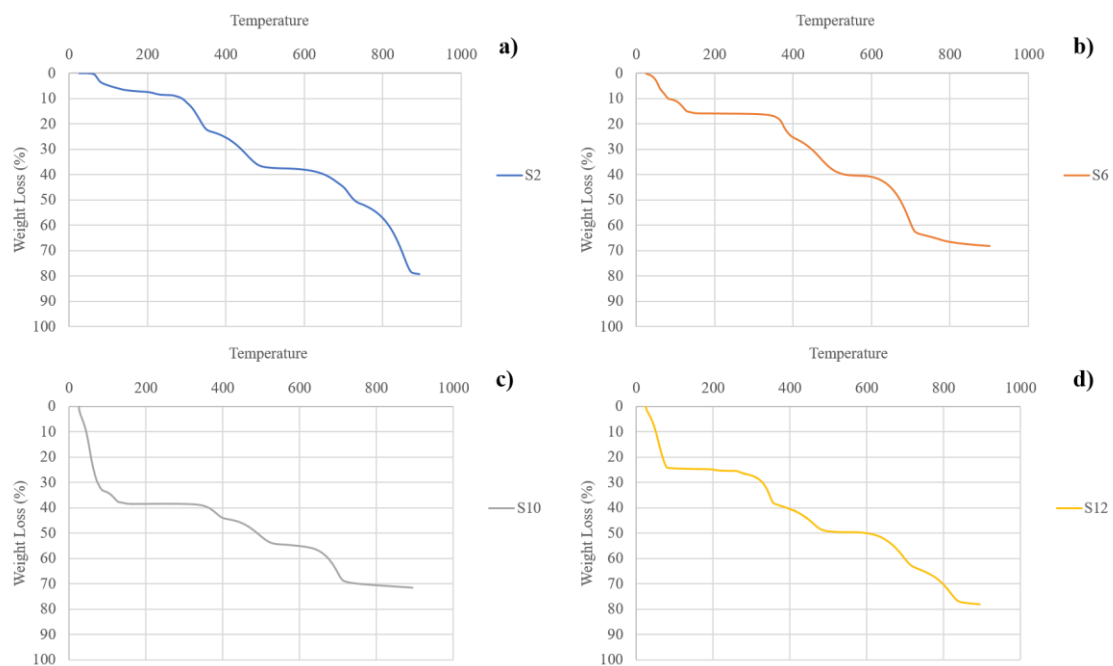
IV – Original TGA curves

Figure E20. Original TGA Curves. Thermograms from a) S2, b) S6, c) S10 and d) S12

Appendix F

Coating properties

I. Coating Properties

To investigate the coating properties of the modified particles, there were made tests to evaluate the ratio starch/PCC most indicated to this process. There were tested three ratios: 1/1, 2/1 and 3/1, and duplicates of each coated paper were made. The 'pick-up' of the coated papers was measured and there were also performed analysis of air permeability (Gurley) and roughness to each paper. Table F1.1, present these values.

Table F1. Ratio Starch/PCC evaluation

Starch/PCC	Pick-up	Air Permeability (s/100mL)	Roughness (mL/min)
1/1	4.4	15.9	296.0
	4.9	18.0	328.8
2/1	5.9	16.1	264.3
	5.1	15.7	239.6
3/1	6.0	15.3	239.7
	6.6	16.5	234.7

II.   Solid content of the coating suspension

Table F2. Percentage of solid content in the coated samples

Samples	Solid Content (wt%)
P-PCC	25.4
	25.4
P-S2	25.4
	25.4
	26.0
	26.0
	26.0
P-S6	26.7
	26.7
	26.0
	26.0
	26.0
P-S10	25.0
	23.9
	23.9
P-S12	26.1
	26.1
	25.3
	25.3